Azimuthally-dependent scattering potentials and full waveform inversion sensitivities in low-loss viscoelastic orthorhombic media

Shahpoor Moradi and Kris Innanen

ABSTRACT

The problem of seismic wave scattering from anisotropic and attenuative inclusions is analyzed within the mathematical framework of the Born approximation. Specifically, a Born scattering model is used to extract scattering potentials, which generalize linearized reflection coefficients and sensitivity kernels, and which in the latter form are a basis for multi-parameter seismic full waveform inversion (FWI) updates. To derive the scattering potentials, a point scatterer comprising a perturbation in each medium property is inserted in a homogeneous isotropic background. The amplitudes, or scattering radiation patterns, associated with incoming and outgoing wave vector pairs provide the weights used to simultaneously invert for viscoelastic and anisotropic medium properties. Analysis of the angle-dependence of the scattering patterns provide qualitative and quantitative insight into inter-parameter trade-offs and cross-talk. We explicitly derive scattering potentials for elastic and viscoelastic P-to-P, P-to-SV and P-to-SH waves in a weak anisotropic, low-loss viscoelastic orthorhombic media. We assume the background or reference medium to be either isotropic-elastic or isotropic-viscoelastic. The results generalize reflection coefficient expressions derived from linearization of exact solutions of the Zoeppritz equation for transversely isotropic viscoelastic media with both vertical (VTI) and horizontal (HTI) axes of symmetry.

INTRODUCTION

The Born approximation is a mathematical framework within which a linearized relationship can be determined between scattered seismic wave fields and the perturbations in medium properties which cause the scattering. Amongst its applications, it provides the sensitivity expressions by which seismic full waveform inversion (FWI) determines simultaneous variations in multiple parameters. Sensitivity, or parameter-resolution, analysis is a key step in determining optimal model parametrization (Gholami et al., 2013b,a), especially in the context of multiparameter updates (Oh and Alkhalifah, 2016a,b; Masmoudi and Alkhalifah, 2016). Some of the earliest discussions of multiparameter FWI predicted that model parameterizations could aggravate or suppress density artifacts (Tarantola, 1986), and in recent field data studies of elastic FWI, slightly different parameterization choices have been shown to lead variously to unambiguous reservoir model estimates which are consistent with rock physics models, or to noisy and un-interpretable results (Pan et al., 2018).

In an isotropic elastic earth model a range of types of parameterization is available, principally involving combinations of density with P and S velocities, P and S impedances or elastic moduli. A study of the radiation patterns induced by each of these models of parameters provide some insights on the most suitable subsurface parameterization for FWI. Recently the influence of the model parameterization on teleseismic FWI for lithospheric imaging has been investigated by Beller et al Beller et al. (2017). Based on the analysis of scattering radiation patterns they concluded that the density model recovered from elastic modulus based parameterization is resolved better than the P and S velocity model and the density model recovered from P and S wave impedances, which are much smoother. Born scattering and FWI model parameterization analyses focusing

on anisotropic media are typically carried out in the acoustic approximation (Plessix and Rynja, 2010; Plessix and Cao, 2011; Masmoudi and Alkhalifah, 2016). In elastic anisotropic media, the sensitivity of the FWI objective function with respect to model parameters for Vertical Transverse Isotropic (VTI) media was analyzed by Kamath and Tsvankin Kamath and Tsvankin (2016). To understand the possible leakage and trade off between the model parameters when the seismic data mainly contain reflection data from horizontal layers, He and Plessix He and Plessix (2017) investigated parameterization selection for compressional body waves in elastic VTI media.

For the case of a viscoelastic background, there are three main types of waves, classified by Borcherdt Borcherdt (2009) as P-wave, S-type I (SI) and S-type II (SII) waves. The polarization and slowness vectors for viscoelastic waves are complex, which in turn lead to complex scattering potentials. Within the Born approximation, the problem of scattering of viscoelastic seismic waves by heterogeneities in both isotropic and anisotropic viscoelastic media has been investigated (Moradi and Innanen, 2015, 2017).

In a series of paper by Bakulin, the seismic characterization of naturally fractured reservoirs was investigated in various types of anisotropic media, including single vertical fracture systems within an isotropic background rock (HTI media)(Bakulin et al., 2000a), two orthogonal fracture sets in an isotropic host rock (orthorhombic media)(Bakulin et al., 2000b), and media with two nonorthogonal sets of rotationally invariant fractures (monoclinic media)(Bakulin et al., 2000c). Fracture characterization of this kind plays a significant role in determining fluid flow during hydrocarbon production (Far, 2011; Far et al., 2013a; Chen et al., 2018). The effects of natural fractures on azimuthal variations in reflected compressional wave-to-compressional wave (hereafter PP) data has been extensively investigated, for fractured gas sands (Sayers and Rickett, 1997), and reservoirs containing multiple fracture sets (Sayers and Dean, 2001) and non-orthogonal fracture sets (Sayers, 2009; Far et al., 2013b). It has been shown that reflection amplitude variations with offset and azimuth for converted PS-waves can reveal more information relevant to reservoir characterization than does the PP-wave reflection amplitudes (Far and Hardage, 2016).

Amplitude variation with offset (AVO) and amplitude-variation-with-azimuth (AVAz) are broadly applied seismic amplitude analysis techniques applied in quantitative reservoir characterization, parameter imaging and migration/inversion (Tsvankin et al., 2010; Castagna and Backus, 1993). The generalization of the AVO equations to encompass volume/point scattering (Stolt and Weglein, 2012) connects them, furthermore, to multi-parameter sensitivity calculations in full waveform inversion, or FWI (Innanen, 2014). The management and use of seismic attenuation in both AVO-AVAz (Chapman et al., 2006; Innanen, 2011; Wu et al., 2014; Behura and Tsvankin, 2009; Chen et al., 2018) and elastic-anisotropic FWI (Burridge et al., 1998; Causse et al., 1999; Charara et al., 2000; Pan et al., 2016, 2017; Fichtner, 2010; Fichtner and van Driel, 2014; Hak and Mulder, 2011; Métivier et al., 2015; da Silva et al., 2016; Yang et al., 2016; Kamei and Pratt, 2013; Keating and Innanen, 2017) is an important and complicating issue. Media which exhibit both viscoelastic and anisotropic features simultaneously are significantly more challenging to quantitatively describe than their elastic-anisotropic counterparts, and are only beginning to receive attention (Carcione et al., 1998; Bai and Tsvankin, 2016; Bai et al., 2017).

The research summarized in this paper is part of an effort to derive interpretable and useable formulas for both AVO-AVAz and full waveform inversion (FWI) sensitivity analysis, in the presence of anisotropy and attenuation. The FWI and AVO goals can be accomplished more or less

simultaneously because of the close connections that can be found between linearized reflection coefficients, e.g., the Aki-Richards approximation (Aki and Richards, 2002), scattering potentials (Stolt and Weglein, 2012), and FWI sensitivity kernels (Tarantola, 1986; Fichtner, 2010). The problem of volume scattering from viscoelastic-anisotropic inclusions alone is of interest, and contains some almost entirely unexplored features, but it lends itself well to the double task of AVO/FWI sensitivity determination. We begin by setting up a scattering framework to describe the interaction of seismic waves with arbitrary perturbations in viscoelastic orthorhombic media. We consider two cases. First, we assume that the reference wave field propagates in an isotropic-elastic background medium, and is scattered by general viscoelastic-orthorhombic perturbations. The planar interface/specular reflection analog of this involves an isotropic-elastic upper half-space and an orthorhombic lower half-space. Second, we assume that the background medium is isotropic-viscoelastic, and that waves scatter from viscoelastic-orthorhombic perturbations. In both cases we analytically examine the relationship between the scattering potentials and the results of linearization of the exact anisotropic-viscoelastic Zoeppritz equations. We show that the former reduce to the latter.

VISCOELASTIC ORTHORHOMBIC MEDIA

The most common model of orthorhombic symmetry involves parallel vertical fractures embedded in a vertical transversely isotropic (VTI) background. The stiffness matrix for an elastic orthorhombic medium has six diagonal element $C_{ii}, i = 1, 2, ..., 6$ and three off diagonal elements C_{12}, C_{13} and C_{23}. If the medium is attenuative, the stiffness tensor is complex, with an imaginary part related to attenuation. The imaginary part is parameterized by a set of quality factors, $Q_{ij} = C_{ij}/C_{ij}^{\mathrm{Im}}$, where C_{ij} and C_{ij}^{Im} are real and imaginary parts of the stiffness tensor components; each independent component of the stiffness tensor has a corresponding quality factor. Which, and how many, of these parameters can be practically constrained in FWI or AVO settings is presently unclear. But, in both cases, quantification of scattering, whether from point or planar perturbations, is the first step in providing answers to such questions. The most useful parameterization is based on the assumption of weak-anisotropy. The real part of the stiffness tensor is characterized by P- and S-wave velocities and seven Thomsen parameters, and the imaginary part by P- and S-wave quality factors and seven Q-dependent anisotropic parameters (Appendix). Thomsen Thomsen (1986) originally defined three parameters to characterize weakly-anisotropic media with a vertical or horizontal axis of symmetry. These parameters vanish in isotropic media as the result of the symmetry of the stiffness tensor. For orthorhombic media with symmetries in x-z and y-z planes, the anisotropy is analogously characterized by seven dimensionless parameters. These parameters reduce to the original three in the VTI/HTI limiting case (Tsvankin, 1997). Ultimately, the stiffness tensor components are defined in terms of anisotropic parameters as

$$
\begin{aligned}
C_{22} &= C_{33}\left(1+2\varepsilon^{(1)}\right),\\
C_{11} &= C_{33}\left(1+2\varepsilon^{(2)}\right),\\
C_{66} &= \frac{1}{2}(C_{55}+C_{44})+\gamma^{(1)}C_{55}+\gamma^{(2)}C_{44},\\
C_{23} &= \sqrt{2\delta^{(1)}C_{33}(C_{33}-C_{44})+(C_{33}-C_{44})^2}-C_{44} \approx C_{33}\left(1+\delta^{(1)}\right)-2C_{44},\\
C_{13} &= \sqrt{2\delta^{(2)}C_{33}(C_{33}-C_{55})+(C_{33}-C_{55})^2}-C_{55} \approx C_{33}\left(1+\delta^{(2)}\right)-2C_{55},\\
C_{12} &= \sqrt{2\delta^{(3)}C_{11}(C_{11}-C_{66})+(C_{11}-C_{66})^2}-C_{66} \approx C_{11}\left(1+\delta^{(3)}\right)-2C_{66}.
\end{aligned}
\tag{1}
$$

Where we have linearized C_{23}, C_{13} and C_{12} respectively in terms of anisotropic parameters $\delta^{(1)}$, $\delta^{(2)}$ and $\delta^{(3)}$ based on the assumption of weak anisotropy. In attenuative media, the same definitions apply, but with the C_{ij} replaced by complex $\hat{C}_{ij}$. Here the Thomsen parameters are complex with real and imaginary parts connected to what are referred to as the anisotropic-viscoelastic Thomsen parameters (Appendix).

SCATTERING POTENTIALS

The main assumption behind the Born approximation states that the actual medium where the wave propagates in it, slightly differs from a homogeneous background medium. The difference between the actual and background media represents the small perturbations of the medium. An elastic homogeneous model of background medium is characterized by its density ρ^0 and its stiffness tensor $C^{(0)}_{ijkl}$, such that the actual medium properties can be written as

$$\rho = \rho_0 + \Delta\rho, \tag{2}$$

$$C_{ijkl} = C^{(0)}_{ijkl} + \Delta C_{ijkl}. \tag{3}$$

The Born approximation assumption is equivalent to $\Delta\rho \ll \rho, \rho_0$ and $\Delta C_{ijkl} \ll C^{(0)}_{ijkl}, C_{ijkl}$. Wave propagation is described by the Green's function or propagator. The scattered wave, which is the difference between the waves propagating in the background and perturbed media, is expanded as a series. The first term of the series describes the sum of all instances of single scattering from the tensor potential. The scattered wave field can be expressed as the quantity scattering potential S (Beylkin and Burridge, 1990)(Appendix)

$$\mathrm{S} = (\boldsymbol{\mathcal{S}}\cdot\boldsymbol{\mathcal{I}})\frac{\Delta\rho}{\rho_0} - \eta_{mn}\frac{\Delta C_{mn}}{\rho_0} = (\boldsymbol{\mathcal{S}}\cdot\boldsymbol{\mathcal{I}})\frac{\Delta\rho}{\rho_0} - (\mathcal{S}_i \mathrm{k}^{\mathrm{Sc}}_j \mathcal{I}_k \mathrm{k}^{\mathrm{In}}_l)\frac{\Delta C_{ijkl}}{\rho_0}, \tag{4}$$

where $\boldsymbol{\mathcal{S}}$ and $\boldsymbol{\mathcal{I}}$ are the scattered and incident polarizations, and $\mathbf{k}^{\mathrm{Sc}}$ and $\mathbf{k}^{\mathrm{In}}$ are the scattered and incident slowness vectors emerging from the application of the derivatives in equation (44) to the Green functions. In addition, $m = ij$ and $n = kl$ are the Voigt indices, with $11 \rightarrow 1, 22 \rightarrow 2, 33 \rightarrow 3, (23, 32) \rightarrow 4, (13, 31) \rightarrow 5, (12, 21) \rightarrow 6$. Figure 1a illustrates the geometry of the point scattering at location $\mathbf{x}$ inserted in a homogeneous background medium. The source is positioned at a location $\mathbf{x}_s$, and the receiver is located at $\mathbf{x}_r$ above the scatter point. The vector $\mathbf{k}^{\mathrm{In}}$ is the slowness vector that is tangent to the ray connecting the source point $\mathbf{x}_s$ to the scatter point $\mathbf{x}$, whereas $\mathbf{k}^{\mathrm{Sc}}$ is the vector that is tangent to the ray connecting the scatter point to the receiver point $\mathbf{x}_r$. The incident (scattered) angle θ_{In} (θ_{Sc}) is defined as an angle between the incident(scattered)

slowness vector $\mathbf{k}^{\mathrm{In}}(\mathbf{k}^{\mathrm{Sc}})$ and $\mathbf{k} = \mathbf{k}^{\mathrm{In}} - \mathbf{k}^{\mathrm{Sc}}$. The sum of incident and scattered angles is called opening angle or scattering angle. Two slowness vectors $\mathbf{k}^{\mathrm{In}}$ and $\mathbf{k}^{\mathrm{Sc}}$ define a scattering plane that makes the azimuth angle φ with respect to the x-axis.

The derivation of scattering potential is given in Appendix . To expose the effects of anisotropy on radiation patterns, we express the perturbation in the stiffness tensor in terms of the perturbations in both viscoelastic and anisotropic parameters. In the case of a background medium that is isotropic and elastic, we have

$$\begin{aligned}
\Delta C_{11} &= \Delta C_{33} + 2C_{33}^{(0)}\varepsilon^{(2)},\\
\Delta C_{22} &= \Delta C_{33} + 2C_{33}^{(0)}\varepsilon^{(1)},\\
\Delta C_{66} &= \frac{1}{2}(\Delta C_{55} + \Delta C_{44}) + C_{55}^{(0)}\left[\gamma^{(1)} + \gamma^{(2)}\right],\\
\Delta C_{23} &= \Delta C_{33} - 2\Delta C_{44} + C_{33}^{(0)}\delta^{(1)},\\
\Delta C_{13} &= \Delta C_{33} - 2\Delta C_{55} + C_{33}^{(0)}\delta^{(2)},\\
\Delta C_{12} &= \Delta C_{33} - (\Delta C_{55} + \Delta C_{44}) + C_{33}^{(0)}\left[\delta^{(3)} + 2\varepsilon^{(2)}\right] - 2C_{55}^{(0)}\left[\gamma^{(1)} + \gamma^{(2)}\right].
\end{aligned} \tag{5}$$

Figure 1a illustrate the configuration of the two model parametrization for orthorhombic media. Each model is decomposed into a background medium with scattering points. One model parametrization is based on the stiffness tensor and the other based on the anisotropic Thomsen parameters. In this paper, we consider a homogeneous isotropic background such that the perturbations in anisotropic parameters are the anisotropic Thomsen parameters in actual medium. This assumption makes our analysis more simpler since we can use the isotropic slowness and polarization vectors rather than their complicated counterparts in anisotropic media. Inserting equation (5) into equation (4), we obtain the general form of the scattering potential

$$\begin{aligned}
\mathrm{S} =& [\rho]\frac{\Delta\rho}{\rho_0} - [C_{33}]\frac{\Delta C_{33}}{\rho_0} - [C_{44}]\frac{\Delta C_{44}}{\rho_0} - [C_{55}]\frac{\Delta C_{55}}{\rho_0}\\
&- [\gamma^{(1)}]\gamma^{(1)} - [\gamma^{(2)}]\gamma^{(2)} - [\varepsilon^{(1)}]\varepsilon^{(1)} - [\varepsilon^{(2)}]\varepsilon^{(2)} - [\delta^{(1)}]\delta^{(1)} - [\delta^{(2)}]\delta^{(2)} - [\delta^{(3)}]\delta^{(3)}.
\end{aligned} \tag{6}$$

Where the straight bracket $[...]$ denotes the sensitivity of scattering potential to each parameter

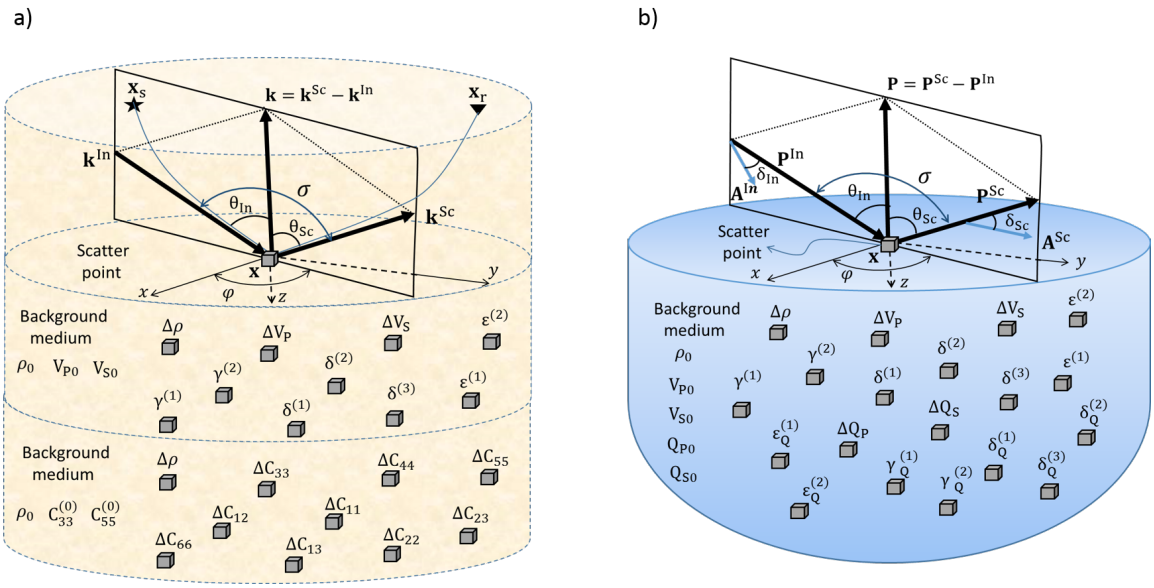

FIG. 1. a) Schematic description of Born scattering. Background medium is characterized by ρ_0 and $C_{ijkl}^{(0)}$; $\mathbf{x}$ is the location of the scatter point; $\mathbf{x}_s$ and $\mathbf{x}_r$ respectively are the location of source and receiver; $\mathbf{k}^{\mathrm{In}}$ is the slowness vector for incident ray and $\mathbf{k}^{\mathrm{Sc}}$ slowness vector for scattered ray; $\mathbf{k}$, is the difference of incident and scattered slowness vectors and these three vectors define the scattering plane; θ^{In}, the angle between $\mathbf{k}^{\mathrm{In}}$ and $\mathbf{k}$ is incident angle; θ^{Sc}, the angle between $\mathbf{k}^{\mathrm{Sc}}$ and $\mathbf{k}$ is the scattered angle; angle between $\mathbf{k}^{\mathrm{Sc}}$ and $\mathbf{k}$ is scattered angle, σ, the angle between $\mathbf{k}^{\mathrm{In}}$ and $\mathbf{k}^{\mathrm{Sc}}$ is the opening angle. The bottom of Figure a is the schematic illustration of breakdown of the orthorhombic media into isotropic background medium and differences in medium properties for Thomsen (top) and stiffness tensor model parametrization (bottom). b) Viscoelastic orthorhombic volume scattering model. $\mathbf{P}_{\mathrm{In}}$ is the incident propagation vector; $\mathbf{P}_{\mathrm{Sc}}$ is the reflected(scattered) propagation vector; $\mathbf{A}_{\mathrm{In}}$ is the incident attenuation vector; $\mathbf{A}_{\mathrm{Sc}}$ is the scattered attenuation vector; δ_{In} is the incident attenuation angle and δ_{Sc} is the scattered attenuation angle.

$$
\begin{aligned}
[\rho] =& \boldsymbol{\mathcal{S}} \cdot \boldsymbol{\mathcal{I}}, \\
[C_{33}] =& (\boldsymbol{\mathcal{S}} \cdot \mathbf{k}^{\mathrm{Sc}})(\boldsymbol{\mathcal{I}} \cdot \mathbf{k}^{\mathrm{In}}), \\
[C_{55}] =& -(\mathcal{S}_1 \mathrm{k}_1^{\mathrm{Sc}} \mathcal{I}_2 \mathrm{k}_2^{\mathrm{In}} + \mathcal{S}_2 \mathrm{k}_2^{\mathrm{Sc}} \mathcal{I}_1 \mathrm{k}_1^{\mathrm{In}}) - 2(\mathcal{S}_1 \mathrm{k}_1^{\mathrm{Sc}} \mathcal{I}_3 \mathrm{k}_3^{\mathrm{In}} + \mathcal{S}_3 \mathrm{k}_3^{\mathrm{Sc}} \mathcal{I}_1 \mathrm{k}_1^{\mathrm{In}}) \\
& + (\mathcal{S}_1 \mathrm{k}_3^{\mathrm{Sc}} + \mathcal{S}_3 \mathrm{k}_1^{\mathrm{Sc}})(\mathcal{I}_1 \mathrm{k}_3^{\mathrm{In}} + \mathcal{I}_3 \mathrm{k}_1^{\mathrm{In}}), + \frac{1}{2}(\mathcal{S}_1 \mathrm{k}_2^{\mathrm{Sc}} + \mathcal{S}_2 \mathrm{k}_1^{\mathrm{Sc}})(\mathcal{I}_1 \mathrm{k}_2^{\mathrm{In}} + \mathcal{I}_2 \mathrm{k}_1^{\mathrm{In}}) \\
[C_{44}] =& -(\mathcal{S}_1 \mathrm{k}_1^{\mathrm{Sc}} \mathcal{I}_2 \mathrm{k}_2^{\mathrm{In}} + \mathcal{S}_2 \mathrm{k}_2^{\mathrm{Sc}} \mathcal{I}_1 \mathrm{k}_1^{\mathrm{In}}) - 2(\mathcal{S}_2 \mathrm{k}_2^{\mathrm{Sc}} \mathcal{I}_3 \mathrm{k}_3^{\mathrm{In}} + \mathcal{S}_3 \mathrm{k}_3^{\mathrm{Sc}} \mathcal{I}_2 \mathrm{k}_2^{\mathrm{In}}) \\
& + (\mathcal{S}_2 \mathrm{k}_3^{\mathrm{Sc}} + \mathcal{S}_3 \mathrm{k}_2^{\mathrm{Sc}})(\mathcal{I}_2 \mathrm{k}_3^{\mathrm{In}} + \mathcal{I}_3 \mathrm{k}_2^{\mathrm{In}}) + \frac{1}{2}(\mathcal{S}_1 \mathrm{k}_2^{\mathrm{Sc}} + \mathcal{S}_2 \mathrm{k}_1^{\mathrm{Sc}})(\mathcal{I}_1 \mathrm{k}_2^{\mathrm{In}} + \mathcal{I}_2 \mathrm{k}_1^{\mathrm{In}}), \\
[\gamma^{(1)}] =& [\gamma^{(2)}] = \mathrm{V}_{\mathrm{S0}}^2 \left[(\mathcal{S}_1 \mathrm{k}_2^{\mathrm{Sc}} + \mathcal{S}_2 \mathrm{k}_1^{\mathrm{Sc}})(\mathcal{I}_1 \mathrm{k}_2^{\mathrm{In}} + \mathcal{I}_2 \mathrm{k}_1^{\mathrm{In}}) - 2\mathcal{S}_1 \mathrm{k}_1^{\mathrm{Sc}} \mathcal{I}_2 \mathrm{k}_2^{\mathrm{In}} - 2\mathcal{S}_2 \mathrm{k}_2^{\mathrm{Sc}} \mathcal{I}_1 \mathrm{k}_1^{\mathrm{In}} \right], \\
[\varepsilon^{(1)}] =& 2\mathrm{V}_{\mathrm{P0}}^2 \mathcal{S}_2 \mathrm{k}_2^{\mathrm{Sc}} \mathcal{I}_2 \mathrm{k}_2^{\mathrm{In}}, \\
[\varepsilon^{(2)}] =& 2\mathrm{V}_{\mathrm{P0}}^2 \left(\mathcal{S}_1 \mathrm{k}_1^{\mathrm{Sc}} \mathcal{I}_1 \mathrm{k}_1^{\mathrm{In}} + \mathcal{S}_1 \mathrm{k}_1^{\mathrm{Sc}} \mathcal{I}_2 \mathrm{k}_2^{\mathrm{In}} + \mathcal{S}_2 \mathrm{k}_2^{\mathrm{Sc}} \mathcal{I}_1 \mathrm{k}_1^{\mathrm{In}} \right), \\
[\delta^{(1)}] =& \mathrm{V}_{\mathrm{P0}}^2 \left(\mathcal{S}_2 \mathrm{k}_2^{\mathrm{Sc}} \mathcal{I}_3 \mathrm{k}_3^{\mathrm{In}} + \mathcal{S}_3 \mathrm{k}_3^{\mathrm{Sc}} \mathcal{I}_2 \mathrm{k}_2^{\mathrm{In}} \right), \\
[\delta^{(2)}] =& \mathrm{V}_{\mathrm{P0}}^2 \left(\mathcal{S}_1 \mathrm{k}_1^{\mathrm{Sc}} \mathcal{I}_3 \mathrm{k}_3^{\mathrm{In}} + \mathcal{S}_3 \mathrm{k}_3^{\mathrm{Sc}} \mathcal{I}_1 \mathrm{k}_1^{\mathrm{In}} \right), \\
[\delta^{(3)}] =& \mathrm{V}_{\mathrm{P0}}^2 \left(\mathcal{S}_1 \mathrm{k}_1^{\mathrm{Sc}} \mathcal{I}_2 \mathrm{k}_2^{\mathrm{In}} + \mathcal{S}_2 \mathrm{k}_2^{\mathrm{Sc}} \mathcal{I}_1 \mathrm{k}_1^{\mathrm{In}} \right).
\end{aligned}
\tag{7}
$$

Since anisotropy is assumed to be week, the difference in C_{44} reduces to

$$
\Delta C_{44} \approx \Delta C_{55} + 2C_{55}^{(0)} \left(\gamma^{(1)} - \gamma^{(2)} \right). \tag{8}
$$

This then generalises the previous expression of scattering potential in equation (6) in terms of the perturbations in density, velocity and anisotropic parameters

$$
\begin{aligned}
\mathrm{S} = & \left\{ [\rho] - [C_{33}] - [C_{44}] - [C_{55}] \right\} \frac{\Delta\rho}{\rho_0} - 2[C_{33}] \frac{\Delta V_{\mathrm{P}}}{V_{\mathrm{P0}}} - 2([C_{44}] + [C_{55}]) \frac{\Delta V_{\mathrm{S}}}{V_{\mathrm{S0}}} \\
& - \left\{ [\gamma^{(1)}] + 2V_{\mathrm{S0}}^2 [C_{44}] \right\} \gamma^{(1)} - \left\{ [\gamma^{(2)}] - 2V_{\mathrm{S0}}^2 [C_{44}] \right\} \gamma^{(2)} \\
& - [\varepsilon^{(1)}] \varepsilon^{(1)} - [\varepsilon^{(2)}] \varepsilon^{(2)} - [\delta^{(1)}] \delta^{(1)} - [\delta^{(2)}] \delta^{(2)} - [\delta^{(3)}] \delta^{(3)}.
\end{aligned}
\tag{9}
$$

As anisotropy vanishes, the above equation reduces to the scattering potential for an elastic wave traveling in an isotropic elastic medium interacting with perturbations in density and P- and S-wave velocities (Stolt and Weglein, 2012). We have now seen that it is not too hard to measure the sensitivity of the scatter wave to the changes in anisotropic parameters. This simplicity and the high efficiency are the main reasons why Born approximation appear more attractive than the approach based on the solution of the Zoeppritz equation.

Scattering of P-wave to P-wave

First we restrict ourselves to the case of isotropic elastic background filled with perturbations in both elastic and anisotropic properties. The perturbations in isotropic parameters that cause scattering are, then, fractional changes in density $\Delta\rho/\rho = (\rho - \rho_0)/\rho$, P-wave velocity $\Delta V_P/V_P = (V_{\mathrm{P}} - V_{\mathrm{P0}})/V_{\mathrm{P}}$ and S-wave velocity $\Delta V_S/V_S = (V_{\mathrm{S}} - V_{\mathrm{S0}})/V_{\mathrm{S}}$. Because the background medium is isotropic, the anisotropic parameters themselves act as perturbations. The angle between the incident and scattered wavefield, referred to as the opening angle, is denoted by $\sigma_{\mathrm{PP}} = 2\theta_{\mathrm{P}}$. From the results that we obtained in previous section, it follows that the elastic scattering potential for

PP-wave is given by $\mathrm{S}^{\mathrm{E}}_{\mathrm{PP}} = \mathrm{S}^{\mathrm{IE}}_{\mathrm{PP}} + \mathrm{S}^{\mathrm{EA}}_{\mathrm{PP}}$ where the isotropic-elastic (IE) and anisotropic-elastic (AE) parts are

$$\begin{aligned}
\mathrm{S}^{\mathrm{IE}}_{\mathrm{PP}} =& -(1+\cos\sigma_{\mathrm{PP}} - 2V^2_{\mathrm{SP}}\sin^2\sigma_{\mathrm{PP}})A_\rho - 2A_{V_{\mathrm{P}}} + 4V^2_{\mathrm{SP}}\sin^2\sigma_{\mathrm{PP}}A_{V_{\mathrm{S}}},\\
\mathrm{S}^{\mathrm{AE}}_{\mathrm{PP}} =& \left[4V^2_{\mathrm{SP}}\cos^2\varphi(\gamma^{(1)}-\gamma^{(2)}) - 2^{-1}(\sin^2\varphi\delta^{(1)} + \cos^2\varphi\delta^{(2)})\right]\sin^2\sigma_{\mathrm{PP}}\\
&- 2\left[\cos^2\varphi\sin^2\varphi\delta^{(3)} + \sin^4\varphi\varepsilon^{(1)} + \left(\cos^2\varphi + \cos^2\varphi\sin^2\varphi\right)\varepsilon^{(2)}\right]\sin^4\frac{\sigma_{\mathrm{PP}}}{2}.
\end{aligned} \tag{10}$$

Here A_ρ is the fractional perturbation in density, $A_{V_{\mathrm{P}}}$ is the fractional perturbation in the P-wave velocity, $A_{V_{\mathrm{S}}}$ is the fractional perturbation in the S-wave velocity and $\mathrm{V_{SP}} = \mathrm{V_{S0}}/\mathrm{V_{P0}}$. It is apparent that: (1) the anisotropic parameters do not influence the scattered wave for a vertically-incident wave ($\sigma_{\mathrm{PP}} = 0$), and (2) to recover the isotropic scattering potential, one may set the anisotropic parameters to zero.

By inspection of (10), the scattered wave is observed to be sensitive to the difference $\gamma^{(S)} = \gamma^{(1)} - \gamma^{(2)}$ rather than $\gamma^{(1)}$ and $\gamma^{(2)}$ individually. For VTI media, $\varepsilon^{(1)} = \varepsilon^{(2)} = \varepsilon$, $\delta^{(1)} = \delta^{(2)} = \delta$ and $\gamma^{(S)} = \delta^{(3)} = 0$, and as a result the anisotropic part of the scattering potential reduces to (Moradi and Innanen, 2017)

$$\mathrm{S}^{\mathrm{AE}}_{\mathrm{PP,VTI}} = -2\sin^2\frac{\sigma_{\mathrm{PP}}}{2}\delta - 2\sin^4\frac{\sigma_{\mathrm{PP}}}{2}(\varepsilon-\delta). \tag{11}$$

In fact, for small angles of incidence, the second term is negligible compared to the first term, that is, the effect of δ dominates over that of ε. For HTI media, $\varepsilon^{(1)} = 0$, $\varepsilon^{(2)} = \varepsilon^{(V)}$, $\delta^{(1)} = \delta^{(2)} = \delta^{(V)}$ and $\gamma^{(S)} = \gamma$, $\delta^{(1)} = 0$, $\delta^{(2)} = \delta^{(V)}$ and $\delta^{(3)} = \delta^{(V)} - 2\varepsilon^{(V)}$ (Tsvankin, 1997, 1996) so the anisotropic part of the scattering potential reduces to

$$\mathrm{S}^{\mathrm{EA}}_{\mathrm{PP,HTI}} = 2^{-2}\sin^2\sigma_{\mathrm{PP}}\cos^2\varphi\left[8V^2_{\mathrm{SP}}\gamma - \delta^{(V)}\right] - 2\cos^2\varphi\left[\sin^2\varphi\delta^{(V)} + \cos^2\varphi\varepsilon^{(V)}\right]\sin^4\frac{\sigma_{\mathrm{PP}}}{2}. \tag{12}$$

Figure 2 shows the radiation patterns generated by anisotropic parameters inserted in an isotropic background as a function of the scattering angles for different azimuth angle.

Each plot is labeled by the corresponding anisotropic parameter which generate the radiation pattern. In all plots, the scatter point is placed at the center of origin. To determine how azimuth angle affect the radiation pattern, we plot the scattering potentials for different values of azimuth angle. Anisotropic parameter $\delta^{(3)}$ has small influence on the radiation pattern and its influence for azimuth angles 0° and 90° goes to zero. Although the radiation patterns generated by $\delta^{(1)}$ and $\delta^{(2)}$ are similar, they behave differently for different values of azimuth angles.

We have thus far considered only an elastic background. Let us now explicitly include the viscoelastic component of the stiffness tensor components. In Figure 1b, a viscoelastic-orthorhombic medium broken up into an isotropic-viscoelastic background medium with perturbations in both viscoelastic and anisotropic parameters, is illustrated. Perturbations in isotropic parameters, as in the non-attenuating cases, are expressed in terms of fractional changes in density, and P- and S-wave velocities, but now additionally with P- and S-wave quality factors; perturbations in anisotropic parameters are the values of anisotropic and viscoelastic-anisotropic parameters of the actual medium. A key aspect of the viscoelastic extension of the scattering potential is the inclusion of the attenuation angle, which is the angle between the propagation and attenuation vectors (Figure 1b).

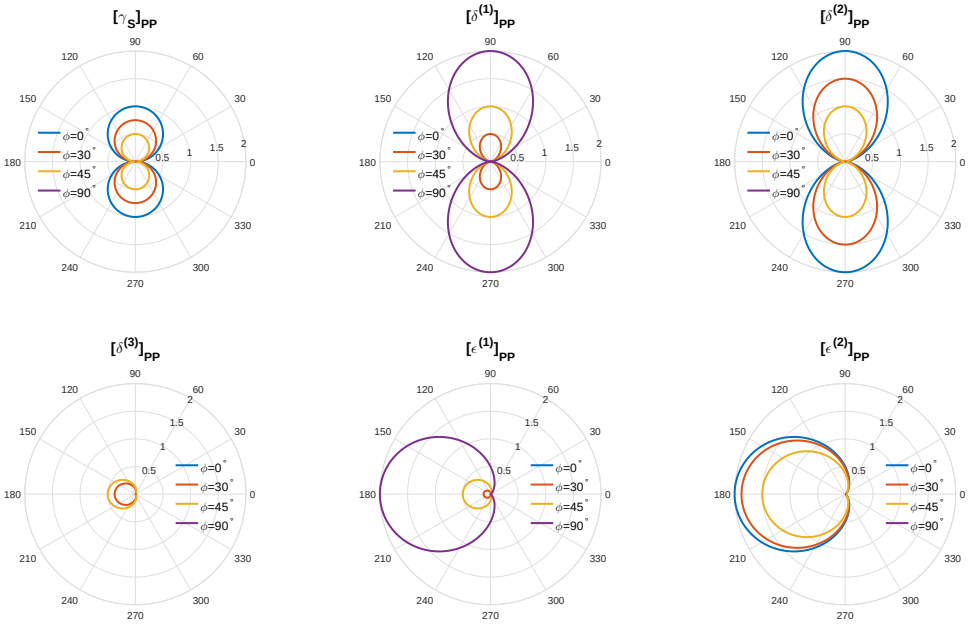

FIG. 2. P-to-P radiation patterns induced by anisotropic parameters versus opening angle $\sigma_{\rm PP} = 2\theta_{\rm P}$ for different values of azimuth angles $\varphi = 0°, 30°, 45°$ and $90°$. The six anisotropic Thomsen parameters are placed into the homogeneous isotropic background with $\rm V_{SP} = V_{S0}/V_{P0} = 1/2$. All plots in this figure are plotted at the same scale.

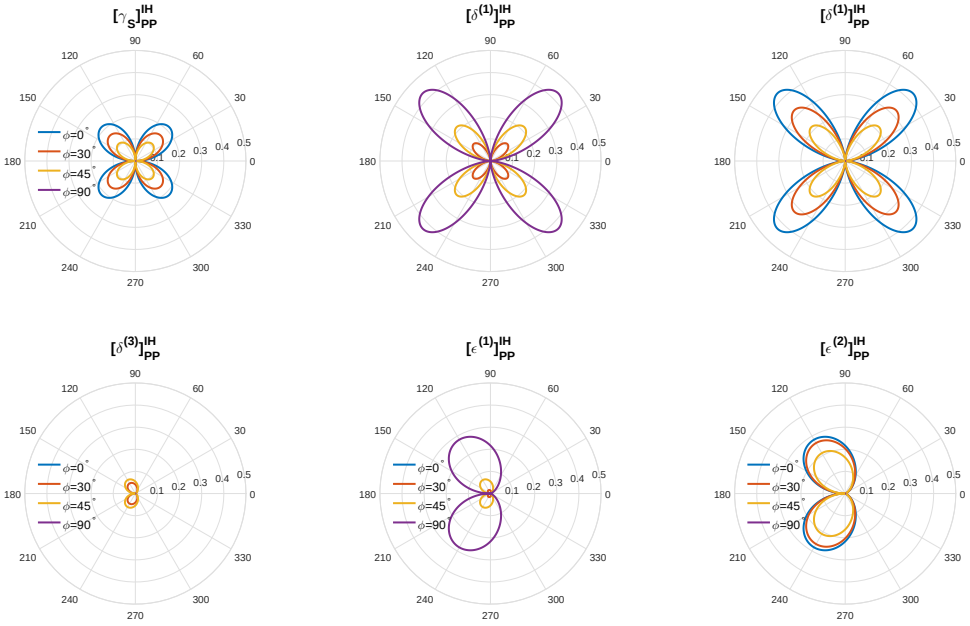

FIG. 3. Inhomogeneous part of the P-to-P scattering potential induced by anisotropic parameters versus opening angle $\sigma_{\rm PP} = 2\theta_{\rm P}$ for different values of azimuth angles $\varphi = 0°, 30°, 45°$ and $90°$. The six anisotropic Thomsen parameters are placed into the homogeneous isotropic background medium with $\rm V_{SP} = V_{S0}/V_{P0} = 1/2$, $\rm Q_{P0} = 10$ and $\rm Q_{S0} = 8$. All plots in this figure are plotted at the same scale.

The anelasticity of the medium supports two classes of waves: those with parallel propagation and attenuation vectors, called homogeneous waves, and those with a non-zero angle between the attenuation and propagation vectors, called inhomogeneous waves. For a homogeneous incident wave we furthermore have $\mathrm{S_{PP}} = \mathrm{S^E_{PP}} + i\mathrm{S^H_{PP}}$, where $\mathrm{S^H_{PP}}$ is the contribution of the anelasticity to the scattering potential (superscript H refers to the homogeneity of the incident wave). This contribution is, in detail,

$$\begin{aligned}\mathrm{S^H_{PP}} =& 2(\mathrm{Q^{-1}_{S0}} - \mathrm{Q^{-1}_{P0}})V^2_{\mathrm{SP}} \sin^2\sigma_{\mathrm{PP}}(A_\rho + 2A_{V_\mathrm{S}}) + \mathrm{Q^{-1}_{P0}}A_{Q_\mathrm{P}} - 2\mathrm{Q^{-1}_{S0}}V^2_{\mathrm{SP}}\sin^2\sigma_{\mathrm{PP}}A_{Q_\mathrm{S}} \\ &+ 2\mathrm{Q^{-1}_{S0}}V^2_{\mathrm{SP}}\sin^2\sigma_{\mathrm{PP}}\cos^2\varphi(\gamma^{(1)}_\mathrm{Q} - \gamma^{(2)}_\mathrm{Q}) - \mathrm{Q^{-1}_{P0}}\sin^2\frac{\sigma_{\mathrm{PP}}}{2}\cos^2\frac{\sigma_{\mathrm{PP}}}{2}(\sin^2\varphi\delta^{(1)}_\mathrm{Q} + \cos^2\varphi\delta^{(2)}_\mathrm{Q}) \\ &- \mathrm{Q^{-1}_{P0}}\sin^4\frac{\sigma_{\mathrm{PP}}}{2}\left[\cos^2\varphi\sin^2\varphi\delta^{(3)}_\mathrm{Q} + \sin^4\varphi\varepsilon^{(1)}_\mathrm{Q} + \left(\cos^2\varphi + \cos^2\varphi\sin^2\varphi\right)\varepsilon^{(2)}_\mathrm{Q}\right].\end{aligned} \tag{13}$$

For incident inhomogeneous wave, scattering potential is given by $\mathrm{S_{PP}} = \mathrm{S^E_{PP}} + i\mathrm{S^H_{PP}} + i\mathrm{S^{IH}_{PP}}$, where contribution of the inhomogeneity of the wave is

$$\begin{aligned}\mathrm{S^{IH}_{PP}} =& \mathrm{Q^{-1}_{P0}}\tan\delta_\mathrm{P}(\sin\sigma_{\mathrm{PP}} + V^2_{\mathrm{SP}}\sin 2\sigma_{\mathrm{PP}})A_\rho + 4V^2_{\mathrm{SP}}\sin 2\sigma_{\mathrm{PP}}A_{V_\mathrm{S}}, \\ &+ \mathrm{Q^{-1}_{P0}}\tan\delta_\mathrm{P}\left[4V^2_{\mathrm{SP}}\cos^2\varphi\gamma^{(S)} - 2^{-1}(\sin^2\varphi\delta^{(1)} + \cos^2\varphi\delta^{(2)})\right]\sin 2\sigma_{\mathrm{PP}} \\ &- 2\mathrm{Q^{-1}_{P0}}\tan\delta_\mathrm{P}\left[\cos^2\varphi\sin^2\varphi\delta^{(3)} + \sin^4\varphi\varepsilon^{(1)} + \left(\cos^2\varphi + \cos^2\varphi\sin^2\varphi\right)\varepsilon^{(2)}\right]\sin^2\frac{\sigma_{\mathrm{PP}}}{2}\sin\sigma_{\mathrm{PP}}.\end{aligned} \tag{14}$$

Where $\delta_\mathrm{P} = \delta^{\mathrm{In}}_\mathrm{P} = \delta^{\mathrm{Sc}}_\mathrm{P}$ is the attenuation angle for either incident or scattered waves. Equation (14) is a function of the fractional change in S-wave velocity, the fractional change in density, and only the non attenuative Thomsen parameters. It is evident that the non attenuative Thomsen parameters influence the imagionary part of the scattering potentials only for inhomogeneous waves. Figure 3 shows the radiation pattern associated with the Thomsen parameters for inhomogeneous incident P-wave. In this figure six Thomsen parameters are inserted in an isotropic viscoelastic background.

Scattering of P-wave to SV-wave

Similar to the P-to-P case, first we consider to the non-attenuative anisotropic medium, and then refine our model by including attenuation as well as inhomogeneity of the wave. Since the background medium is isotropic the scattering potential for converted PSV-wave is given by $\mathrm{S^E_{PSV}} = \mathrm{S^{IE}_{PS}} + \mathrm{S^{AE}_{PS}}$, with the isotropic part

$$\mathrm{S^{IE}_{PSV}} = \left[\sin(\theta_P + \theta_S) + \sin 2(\theta_P + \theta_S)\mathrm{V_{SP}}\right]A_\rho + 2\mathrm{V_{SP}}\sin 2(\theta_P + \theta_S)A_{V_\mathrm{S}},$$

and anisotropic part

$$\mathrm{S^{AE}_{PS}} = \left[\sin 2(\theta_P + \theta_S)\right]\mathrm{N_{PSV1}} + \left[\sin\theta_S\cos\theta_S\right]\mathrm{N_{PSV2}} + \left[\sin^2\theta_P\sin\theta_S\cos\theta_S\right]\mathrm{N_{PSV3}},$$

characterized by azimuth dependent coefficients $\mathrm{N_{PS1}}$, $\mathrm{N_{PS2}}$ and $\mathrm{N_{PS3}}$

$$\begin{aligned}\mathrm{N_{PSV1}} =& 2\mathrm{V_{SP}}\sin^2\varphi\gamma^{(S)}, \\ \mathrm{N_{PSV2}} =& -\mathrm{V_{PS}}(\sin^2\varphi\delta^{(1)} + \cos^2\varphi\delta^{(2)}), \\ \mathrm{N_{PSV3}} =& 2\mathrm{V_{PS}}\left[(\sin^2\varphi\delta^{(1)} + \cos^2\varphi\delta^{(2)}) - \sin^2\varphi\cos^2\varphi\delta^{(3)}\right] \\ &- 2\mathrm{V_{PS}}\left[\sin^4\varphi\varepsilon^{(1)} + \left(\cos^4\varphi + 2\cos^2\varphi\sin^2\varphi\right)\varepsilon^{(2)}\right],\end{aligned}$$

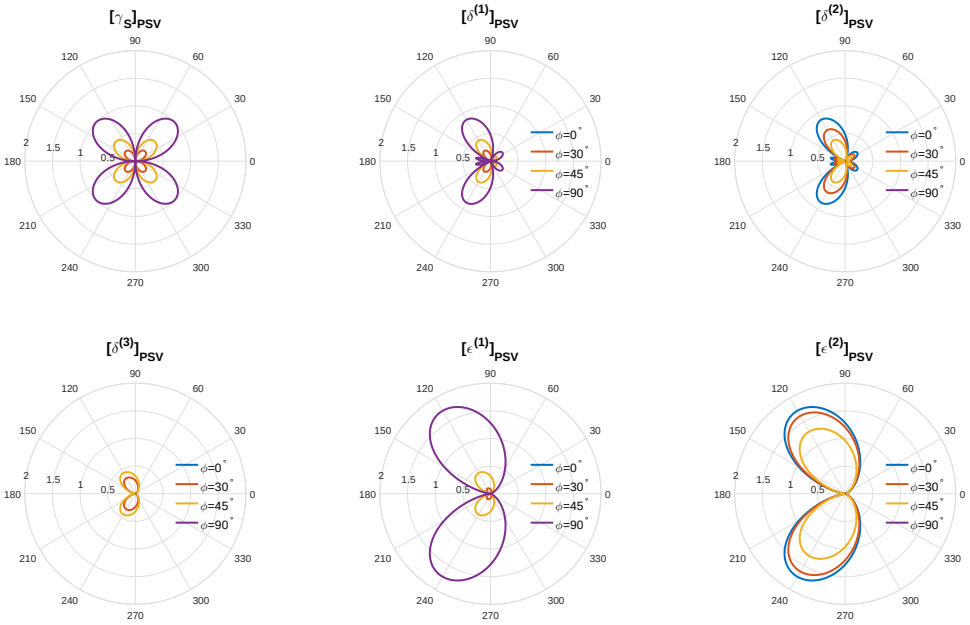

FIG. 4. P-to-SV radiation patterns induced by anisotropic parameters versus opening angle $\sigma_{\rm PS} = (\theta_{\rm P} + \theta_{\rm S})$ for different values of azimuth angles $\varphi = 0°, 30°, 45°$ and $90°$. The six anisotropic Thomsen parameters are placed into the homogeneous isotropic background with $\rm V_{SP} = V_{S0}/V_{P0} = 1/2$. All plots in this figure are plotted at the same scale.

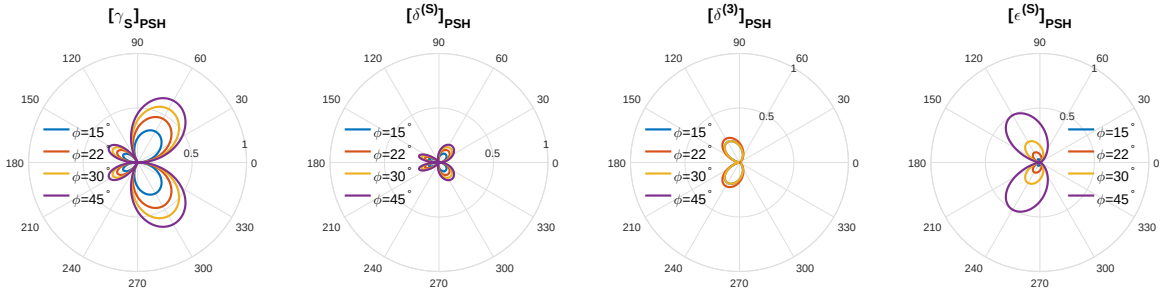

FIG. 5. P-to-SH radiation patterns induced by anisotropic parameters versus opening angle $\sigma_{\rm PS} = (\theta_{\rm P} + \theta_{\rm S})$ for different values of azimuth angles $\varphi = 15°, 22°, 30°$ and $45°$. The six anisotropic Thomsen parameters are placed into the homogeneous isotropic background with $\rm V_{SP} = V_{S0}/V_{P0} = 1/2$. All plots in this figure are plotted at the same scale.

where $\rm V_{PS} = V_{P0}/V_{S0}$. We can see that the isotropic-elastic part of the scattering potential is a function of opening angle between the incident P-waveand scattered SV-wave number, i.e. $(\theta_{\rm P} + \theta_{\rm S})$, however for the anisotropic part only $\gamma^{(\rm S)}$ term varies with opening angle. For incident and scattered waves in opposite directions, where the opening angle is zero, scattering potential is sensitive only to the changes in δ and ε parameters. For a VTI media, the scattering potential reduces to (Moradi and Innanen, 2017)

$$\rm S^{VTI}_{PSV} = S^{IE}_{PSV} - V_{PS}\delta\left[\sin\theta_S\cos\theta_S\right] + 2V_{PS}(\delta-\varepsilon)\left[\sin^2\theta_P\sin\theta_S\cos\theta_S\right]. \tag{15}$$

As it is expected no dependency to the azimuth angle for VTI scattering potential, however for HTI media the scattering potential is azimuth dependent

$$\begin{aligned}\rm S^{HTI}_{PSV} = S^{IE}_{PSV} &+ 2V_{SP}\sin^2\varphi\gamma\left[\sin 2(\theta_P+\theta_S)\right] - V_{PS}\cos^2\varphi\delta^{(V)}\left[\sin\theta_S\cos\theta_S\right]\\ &+ 2V_{PS}\cos^4\varphi(\delta^{(V)}-\varepsilon^{(V)})\left[\sin^2\theta_P\sin\theta_S\cos\theta_S\right].\end{aligned} \tag{16}$$

Figure (4) shows the radiation patterns generated by the six anisotropic scatter points inserted in an isotropic elastic background. Similar to the PP scattering potentials parameter $\delta^{(3)}$ has the minimal infeluence on the scattering potential. The effect of attenuation of medium and inhomogeneity of the wave will be analysed in the next section when we discussed the AVO/Az for converted wave scattering.

Scattering of P-wave to SH-wave

The P-SH converted wave occurs at the anisotropic media when the axis of symmetry is not vertical everywhere. This kind of wave can be observed in teleseismic P-waves (Levin and Park, 1997). For an incident P-wave scattered to the SH wave, the scattering potential is

$$\begin{aligned} \mathrm{S_{PSH}} = & 2\mathrm{V_{SP}} \sin 2\varphi\gamma^{(\mathrm{S})} \left[\cos\theta_{\mathrm{P}} \sin(\theta_P + \theta_S)\right] - \frac{1}{2}\sin 2\varphi\delta^{(S)} \left[\sin\theta_P \cos^2\theta_P\right] \\ & + \frac{1}{2}\sin 2\varphi \left[\left(\sin^2\varphi - \cos^2\varphi\right)\delta^{(3)} - 2\sin^2\varphi\varepsilon^{(S)}\right]\left[\sin^3\theta_P\right], \end{aligned}$$

where $\delta^{(S)} = \delta^{(1)} - \delta^{(2)}$ and $\varepsilon^{(S)} = \varepsilon^{(1)} - \varepsilon^{(2)}$. It is obvious that there is no isotropic term as in an isotropic media P-wave does not scatter to the SH wave. For $(\theta_P + \theta_S) = 0$, where the incident and scatter waves are in opposite direction, the first term goes to zero, which means that the scattering potential is not influenced by $\gamma^{(S)}$ anymore. For a VTI media the scattering potential is zero, however for HTI media we have

$$\begin{aligned} \mathrm{S^{HTI}_{PSH}} = & 2\mathrm{V_{SP}} \sin 2\varphi\gamma \left[\cos\theta_{\mathrm{P}} \sin(\theta_P + \theta_S)\right] + \frac{1}{2}\sin 2\varphi\delta^{(V)} \left[\sin\theta_P \cos^2\theta_P\right] \\ & + \frac{1}{2}\sin 2\varphi \left[\left(\sin^2\varphi - \cos^2\varphi\right)\delta^{(V)} + 2\cos^2\varphi\varepsilon^{(V)}\right]\left[\sin^3\theta_P\right]. \end{aligned}$$

Figure 5 shows the sensitivity of the PSH scattering potential to the anisotropic Thomsen parameters. It is worth noting here that for larger azimuth angles the effects of γ and ε parameters on the scattering potential dominates over δ parameters. We will discuss the effects of attenuation on the scattering in the AVO/Az section.

AMPLITUDE VARIATION WITH OFFSET EQUATIONS

Specular reflection (involving two homogeneous half-spaces separated by a plane boundary) and volume scattering from a point perturbation from a homogeneous background, are asymptotically equivalent with diminishing contrast and opening angle. In our case the corresponding system of isotropic/anisotropic half-spaces involves a low contrast medium with boundary separating an isotropic elastic half-space from an anisotropic elastic medium with weak anisotropic properties. The illustration of the low contrast medium in this study is as follow. The upper layer is an isotropic-elastic medium defined by $(\rho_1, \mathrm{V_{P1}}, \mathrm{V_{S1}})$ in contact with a plane interface separating the upper layer from the anisotropic elastic lower layer defined by $\Big(\rho_2, , \mathrm{V_{P2}}, \mathrm{V_{S2}}, \delta_2^{(1)}, \delta_2^{(2)}, \delta_2^{(3)}, \varepsilon_2^{(1)}, \varepsilon_2^{(2)}, \gamma_2^{(1)}, \gamma_2^{(2)}\Big)$. Fractional changes in isotropic properties are given by the fractional change in P-wave velocity, $\mathrm{A_{V_P}} = \Delta\mathrm{V_P}/\bar{\mathrm{V}}_{\mathrm{P}}$ where $\Delta\mathrm{V_P} = \mathrm{V_{P1}} - \mathrm{V_{P2}}$ and $\bar{\mathrm{V}}_{\mathrm{P}} = (\mathrm{V_{P1}} + \mathrm{V_{P2}})/2$ are respectively the difference and average of the the P-wave velocity in the lower and upper media; fractional changes in S-wave velocity, $\mathrm{A_{V_S}} = \Delta\mathrm{V_S}/\bar{\mathrm{V}}_{\mathrm{S}}$ where $\Delta\mathrm{V_S} = \mathrm{V_{S1}} - \mathrm{V_{S2}}$ and $\bar{\mathrm{V}}_{\mathrm{S}} = (\mathrm{V_{S1}} + \mathrm{V_{S2}})/2$,

and fractional changes in density, $\mathrm{A}_\rho = \Delta\rho/\rho$ where $\Delta\rho = \rho_2 - \rho_1$ and $\rho = (\rho_2 + \rho_1)/2$ (Table 1). Linearizations are performed based on the anisotropic parameters in the lower layer rather than the differences in anisotropic parameters.

The scattering potentials that we obtained in the previous section can be used to obtain the amplitude variation with offset equations previously derived using the linearization of the Zoeppritz equations (Ruger, 1997). This can be seen intuitively from the fact that reflection coefficient is related to the scattering potential by

$$\mathrm{R}^{\mathrm{E}}_{\mathrm{PP}} = -(2\cos\theta_P)^{-2}\mathrm{S}^{\mathrm{E}}_{\mathrm{PP}} = \mathrm{R}^{\mathrm{IE}}_{\mathrm{PP}} + \mathrm{R}^{\mathrm{AE}}_{\mathrm{PP}}, \tag{17}$$

where the isotropic-elastic reflection coefficient is (Aki and Richards, 2002)

$$\mathrm{R}^{\mathrm{IE}}_{\mathrm{PP}} = 2^{-1}\mathrm{A}_{\mathrm{Z_P}} + \left(2^{-1}\mathrm{A}_{\mathrm{V_P}} - 2\mathrm{V}^2_{\mathrm{SP}}\mathrm{A}_\mu\right)\sin^2\theta_P + 2^{-1}\mathrm{A}_{\mathrm{V_P}}\tan^2\theta_P\sin^2\theta_P, \tag{18}$$

and anisotropic elastic reflection coefficient is (Ruger, 1997)

$$\begin{aligned}\mathrm{R}^{\mathrm{AE}}_{\mathrm{PP}} =& 2^{-1}\left\{\delta^{(2)}_2 + \sin^2\varphi\left[\delta^{(1)}_2 - \delta^{(2)}_2 - 8\mathrm{V}^2_{\mathrm{SP}}\gamma^{(S)}_2\right]\right\}\sin^2\theta_P \\ &+ 2^{-1}\left\{\cos^2\varphi\sin^2\varphi\left[\delta^{(3)}_2 + \varepsilon^{(2)}_2 - \varepsilon^{(1)}_2\right] + \sin^2\varphi\left[\varepsilon^{(1)}_2 - \varepsilon^{(2)}_2\right] + \varepsilon^{(2)}_2\right\}\tan^2\theta_P\sin^2\theta_P,\end{aligned} \tag{19}$$

and where $\mathrm{Z_P} = \rho\mathrm{V_P}$ is the P-wave impedance, $\mu = \rho\mathrm{V}^2_{\mathrm{S}}$ is the shear modulus, with the corresponding fractional changes $\mathrm{A}_{\mathrm{Z_P}}$ and A_μ. Equation (19) is the linearized reflection coefficient as commonly expressed in the literature (Ruger, 1997; Vavrycuk and Psencik, 1998; Ruger, 2002) for weak contrast interfaces separating two weakly orthorhombic media. As the incident half-space (i.e., the upper layer) is anisotropic, these authors used the complicated form of the polarization and slowness vectors for incident and reflected waves. After solving of the Zoeppritz equations, the amplitude of the reflected wave is linearized, obtaining equation (19). In our derivation, we used the incident half-space as an isotropic background medium and used the polarizations and velocities for an isotropic media and obtained the same results. We conclude that for a low-contrast medium with two weakly-anisotropic half-spaces the linearized reflection coefficients are the same as those for which the incident half-space is isotropic.

For an isotropic upper half-space over a VTI medium, the anisotropic part of the reflectivity reduces to $2^{-1}(\sin^2\theta_P\tan^2\theta_P\varepsilon_2 + \sin^2\theta_P\delta_2)$. For HTI media, the anisotropic part of the reflectivity reduces to (Ruger, 2002)

$$\begin{aligned}\mathrm{R}^{\mathrm{EA}}_{\mathrm{PP,HTI}} =& 2^{-1}\left(\delta^{(V)}_2\cos^2\varphi - 8\mathrm{V}^2_{\mathrm{SP}}\sin^2\varphi\gamma_2\right)\sin^2\theta_P \\ &+ 2^{-1}\cos^2\varphi\left(\sin^2\varphi\delta^{(V)}_2 + \cos^2\varphi\varepsilon^{(V)}_2\right)\tan^2\theta_P\sin^2\theta_P.\end{aligned} \tag{20}$$

The result in equation (10), which embodies our formulation of the anisotropic scattering potential, is therefore consistent with the previously-derived reflection coefficients for a boundary separating an isotropic medium from an anisotropic medium. In our derivation we have assumed that the actual medium is anisotropic-elastic and decomposable into an isotropic background with perturbations in both elastic and anisotropic parameters for actual medium. This is (within the linearized Zoeppritz solution framework) equivalent to the case of a low contrast planar boundary between an isotropic medium over an anisotropic medium. However, we saw that the linearized reflection coefficients are the same as those for which an anisotropic medium overlies an anisotropic medium, i.e.,

	Volume scattering			Low-contrast reflection		
	Reference medium	Actual medium	Fractional perturbation	Upper layer	Lower layer	Fractional perturbation
Isotropic-Elastic	ρ_0 V_{P0} V_{S0}	ρ V_P V_S	$\frac{\rho-\rho_0}{\rho}$ $\frac{V_S-V_{S0}}{V_S}$ $\frac{V_P-V_{P0}}{V_P}$	ρ_1 V_{P1} V_{S1}	ρ_2 V_{P2} V_{S2}	$\frac{\rho_2-\rho_1}{2(\rho_2+\rho_1)}$ $\frac{V_{P2}-V_{P1}}{2(V_{P2}+V_{P1})}$ $\frac{V_{S2}-V_{S1}}{2(V_{S2}+V_{S1})}$
Isotropic-Viscoelastic	Q_{P0} Q_{S0}	Q_P Q_S	$\frac{Q_P-Q_{P0}}{Q_P}$ $\frac{Q_S-Q_{S0}}{Q_S}$	Q_{P1} Q_{S1}	Q_{P2} Q_{S2}	$\frac{Q_{P2}-Q_{P1}}{2(Q_{P2}+Q_{P1})}$ $\frac{Q_{S2}-Q_{S1}}{2(Q_{S2}+Q_{S1})}$
Anisotropic-Elastic	0	$\varepsilon^{(1)}$ $\delta^{(3)}$ $\varepsilon^{(2)}$ $\gamma^{(1)}$ $\delta^{(1)}$ $\gamma^{(2)}$ $\delta^{(2)}$	$\varepsilon^{(1)}$ $\delta^{(3)}$ $\varepsilon^{(2)}$ $\gamma^{(1)}$ $\delta^{(1)}$ $\gamma^{(2)}$ $\delta^{(2)}$	0	$\varepsilon_2^{(2)}$ $\delta_2^{(3)}$ $\varepsilon_2^{(1)}$ $\gamma_2^{(1)}$ $\delta_2^{(1)}$ $\gamma_2^{(2)}$ $\delta_2^{(2)}$	$\varepsilon_2^{(2)}$ $\delta_2^{(3)}$ $\varepsilon_2^{(1)}$ $\gamma_2^{(1)}$ $\delta_2^{(1)}$ $\gamma_2^{(2)}$ $\delta_2^{(2)}$
Anisotropic-Viscoelastic	0	$\varepsilon_Q^{(1)}$ $\delta_Q^{(3)}$ $\varepsilon_Q^{(2)}$ $\gamma_Q^{(1)}$ $\delta_Q^{(1)}$ $\gamma_Q^{(2)}$ $\delta_Q^{(2)}$	$\varepsilon_Q^{(1)}$ $\delta_Q^{(3)}$ $\varepsilon_Q^{(2)}$ $\gamma_Q^{(1)}$ $\delta_Q^{(1)}$ $\gamma_Q^{(2)}$ $\delta_Q^{(2)}$	0	$\varepsilon_{Q2}^{(1)}$ $\delta_{Q2}^{(3)}$ $\varepsilon_{Q2}^{(2)}$ $\gamma_{Q2}^{(1)}$ $\delta_{Q2}^{(1)}$ $\gamma_{Q2}^{(2)}$ $\delta_{Q2}^{(2)}$	$\varepsilon_{Q2}^{(1)}$ $\delta_{Q2}^{(3)}$ $\varepsilon_{Q2}^{(2)}$ $\gamma_{Q2}^{(1)}$ $\delta_{Q2}^{(1)}$ $\gamma_{Q2}^{(2)}$ $\delta_{Q2}^{(2)}$

Table 1. A table illustrating the perturbation terms used in volume scattering and low-contrast reflectivity models. Medium properties are classified into isotropic-elastic, isotropic-viscoelastic, anisotropic-elastic and anisotropic-viscoelastic. In volume scattering scheme, the actual medium which is anisotropic-viscoelastic splits into the isotropic background medium filled by the perturbations in medium properties. Since the background medium is isotropic, anisotropic parameters in actual medium act as perturbations.

the case that background medium is also anisotropic. If we replace the anisotropic parameters in the lower medium with fractional differences in properties, the linearized reflection coefficient for an orthorhombic medium is obtained. To obtain the first order reflection coefficients in anisotropic media, in other words, we do not need to consider the anisotropic form of the polarizations and slowness vectors. To examine how attenuation influences the scattered, or AVO, response, we consider the two layer model in which the upper layer is isotropic-viscoelastic and lower layer is anisotropic-viscoelastic. The linearized PP reflection coefficient is $\mathrm{R_{PP}} = \mathrm{R^{E}_{PP}} + i\mathrm{R^{H}_{PP}}$, where the contribution due to attenuation is

$$\mathrm{R^{H}_{PP}} = -(2\cos\theta_P)^{-2}\mathrm{S^{H}_{PP}} = \mathrm{A^{H}_{PP}} + \mathrm{B^{H}_{PP}}\sin^2\theta_\mathrm{P} + \mathrm{C^{H}_{PP}}\sin^2\theta_P\tan^2\theta_P, \tag{21}$$

where

$$\begin{aligned}
\mathrm{A^{H}_{PP}} =& -(4\mathrm{Q_{P0}})^{-1}A_{Q_\mathrm{P}}\\
\mathrm{B^{H}_{PP}} =& -2(\mathrm{Q^{-1}_{S0}} - \mathrm{Q^{-1}_{P0}})V^2_\mathrm{SP}A_\mu - (4\mathrm{Q_{P0}})^{-1}A_{Q_\mathrm{P}} + 2\mathrm{Q^{-1}_{S0}}V^2_\mathrm{SP}A_{Q_\mathrm{S}}\\
&- 2\mathrm{Q^{-1}_{S0}}V^2_\mathrm{SP}\cos^2\varphi(\gamma^{(1)}_\mathrm{Q} - \gamma^{(2)}_\mathrm{Q}) + 4^{-1}\mathrm{Q^{-1}_{P0}}(\sin^2\varphi\delta^{(1)}_\mathrm{Q} + \cos^2\varphi\delta^{(2)}_\mathrm{Q}),\\
\mathrm{C^{H}_{PP}} =& -(4\mathrm{Q_{P0}})^{-1}\left\{A_{Q_\mathrm{P}} - \left[\cos^2\varphi\sin^2\varphi\delta^{(3)}_\mathrm{Q} + \sin^4\varphi\varepsilon^{(1)}_\mathrm{Q} + \left(\cos^2\varphi + \cos^2\varphi\sin^2\varphi\right)\varepsilon^{(2)}_\mathrm{Q}\right]\right\}.
\end{aligned} \tag{22}$$

It has been shown that attenuation affects both the intercept and gradient of the linearized PP reflection coefficients in viscoelastic-isotropic media (Moradi and Innanen, 2016; Samec and Blangy, 1992). Analysis of the exact PP reflection coefficient near the critical angle indicates that the attenuation and anisotropy do not affect the normal incident reflectivity (Carcione et al., 1998). Our linearized reflection coefficient forms predict that only the P-wave quality factor influences vertically-incident waves— there is no influence of anisotropic and anisotropic-viscoelastic parameters on the reflection coefficient at normal incidence. In the case that anisotropy goes to zero, our results reduce to the AVO equations PP-waves in low-loss viscoelastic media, for homogeneous incident wave (Moradi and Innanen, 2016).

For incident inhomogeneous waves, the reflectivity formula is $\mathrm{R_{PP}} = \mathrm{R^{E}_{PP}} + i\mathrm{R^{H}_{PP}} + i\mathrm{R^{IH}_{PP}}$, where the contribution of the inhomogeneity of the wave is

$$\begin{aligned}
\mathrm{R^{IH}_{PP}} =& -\mathrm{Q^{-1}_{P0}}\tan\delta_\mathrm{P}\mathrm{V^2_{SP}}\sin 2\theta_P\mathrm{A}_\mu + 2^{-1}\mathrm{Q^{-1}_{P0}}\tan\delta_\mathrm{P}\tan\theta_P(1+\tan^2\theta_P)\mathrm{A_{Vp}}\\
&+ 4^{-1}\mathrm{Q^{-1}_{P0}}\tan\delta_\mathrm{P}\left(\delta^{(2)}_2 + \sin^2\varphi\left[\delta^{(1)}_2 - \delta^{(2)}_2 - 8\mathrm{V^2_{SP}}\gamma^{(S)}_2\right]\right)\sin 2\theta_P\\
&+ 2^{-1}\mathrm{Q^{-1}_{P0}}\tan\delta_\mathrm{P}\left(\cos^2\varphi\sin^2\varphi(\delta^{(3)}_2 + \varepsilon^{(2)}_2 - \varepsilon^{(1)}_2) + \sin^2\varphi(\varepsilon^{(1)}_2 - \varepsilon^{(2)}_2) + \varepsilon^{(2)}_2\right)\tan^3\theta_P.
\end{aligned}$$

At normal incidence, the inhomogeneity of the wave has no effect on the reflectivity. This term is controlled by changes in density, P- and S-wave velocity and anisotropic parameters $\delta^{(2)}$, $\varepsilon^{(2)}$ and $\gamma^{(S)}$. It is not sensitive into the changes in P- and S-wave quality factors, nor is it sensitive to changes in anisotropic-viscoelastic parameters. For azimuth angle $\varphi = 0°$, the inhomogeneous part of the reflection coefficient is sensitive only to $\delta^{(2)}$, however it doesn't have any effect on reflectivity for azimuth angle $\varphi = 90°$. To derive the linearized reflection coefficients for converted PSV and PSH we use the relationship between the scattering potential and reflection coefficient (Moradi and Innanen, 2016)

$$\mathrm{R_{PS}} = \frac{\sin\theta_\mathrm{P}}{\cos\theta_\mathrm{S}\sin(\theta_\mathrm{P}+\theta_\mathrm{S})}\mathrm{S_{PS}} = \mathrm{R^{IE}_{PS}} + \mathrm{R^{AE}_{PS}}.$$

For PSV wave, the isotropic-elastic part of the reflectivity is given by

$$\mathrm{R}_{\mathrm{PSV}}^{\mathrm{IE}} = -\frac{1}{2}\frac{\Delta\rho}{\bar{\rho}}\left[\frac{\sin\theta_P}{\cos\theta_S}\right] - \frac{V_S}{V_P}\mathrm{A}_\mu\left[\sin\theta_P\cos\theta_S\right] + \left(\frac{V_S}{V_P}\right)^2\mathrm{A}_\mu\left[\frac{\sin^3\theta_P}{\cos\theta_S}\right].$$

Additionally the anisotropic-elastic part

$$\begin{aligned}\mathrm{R}_{\mathrm{PSV}}^{\mathrm{AE}} = \mathrm{A}_{\mathrm{PSV1}}^{\mathrm{AE}}\left[\frac{\sin\theta_P}{\cos\theta_S}\right] + \mathrm{A}_{\mathrm{PSV2}}^{\mathrm{AE}}\left[\cos\theta_P\sin\theta_P\right] + \mathrm{A}_{\mathrm{PSV3}}^{\mathrm{AE}}\left[\frac{\sin^3\theta_P}{\cos\theta_S}\right] \\ + \mathrm{A}_{\mathrm{PSV4}}^{\mathrm{AE}}\left[\cos\theta_P\sin^3\theta_P\right] + \mathrm{A}_{\mathrm{PSV5}}^{\mathrm{AE}}\left[\frac{\sin^5\theta_P}{\cos\theta_S}\right].\end{aligned} \tag{23}$$

With coefficients depend to P- and S-wave velocity and anisotropic Thomsen parameters (Appendix). If the incident half-space where the incident wave propagates is anisotropic, the values on the anisotropic parameters in lower layer is replaced by the contrasts between the anisotropic parameters (Jílek, 2002b,a). On the other hand if the incident half-space is anisotropic and the lower layer is isotropic, the reflection coefficients are the same as eq.(23) with opposite signs of the anisotropic parameters. Our results in the case that the lower medium is VTI/HTI coincides to the approximate converted PSV reflection coefficients derived by Rüger Ruger (2002). For normal incident of angle in contrast to the PP case, both isotropic and anisotropic terms go to zero. Now let us consider to the case that the background medium is isotropic-viscoelastic. This is equivalent to the low-contrast medium with isotropic-viscoelastic top layer over a viscoelastic-orthorhombic media. In this case an imaginary term added to the scattering potential and consequently to the reflectivity which can be break into two terms

$$\begin{aligned}\mathrm{R}_{\mathrm{PSV}}^{\mathrm{H}} =&\mathrm{A}_{\mathrm{PSV1}}^{\mathrm{H}}\left[\frac{\sin\theta_P}{\cos\theta_S}\right] + \mathrm{A}_{\mathrm{PSV2}}^{\mathrm{H}}\left[\cos\theta_P\sin\theta_P\right] + \mathrm{A}_{\mathrm{PSV3}}^{\mathrm{H}}\left[\frac{\sin^3\theta_P}{\cos\theta_S}\right] \\ &+ \mathrm{A}_{\mathrm{PSV4}}^{\mathrm{H}}\left[\cos\theta_P\sin^3\theta_P\right] + \mathrm{A}_{\mathrm{PSV5}}^{\mathrm{H}}\left[\frac{\sin^5\theta_P}{\cos\theta_S}\right],\end{aligned} \tag{24}$$

$$\mathrm{R}_{\mathrm{PSV}}^{\mathrm{IH}} = \mathrm{A}_{\mathrm{PSV1}}^{\mathrm{IH}} + \mathrm{A}_{\mathrm{PSV2}}^{\mathrm{IH}}\sin^2\theta_P + \mathrm{A}_{\mathrm{PSV3}}^{\mathrm{IH}}\sin^4\theta_P + \mathrm{A}_{\mathrm{PSV4}}^{\mathrm{IH}}\sin^6\theta_P. \tag{25}$$

For homogeneous part, the coefficients (Appendix) are the function of P- and S-wave velocity, P- and S-wave quality factors and Q-dependent Thomsen parameters, dependency of this term to the P- and S-wave angles is the same as anisotropic term in eq. (23). For very small angles of incidence the first two term dominates over other terms, which means that reflectivity depends to the $\gamma^{(\mathrm{S})}$, $\delta^{(1)}$ and $\delta^{(2)}$ and corresponding Q-dependant Thomsen parameters $\gamma_{\mathrm{Q}}^{(\mathrm{S})}$, $\delta_{\mathrm{Q}}^{(1)}$ and $\delta_{\mathrm{Q}}^{(2)}$.

On the other hand for inhomogeneous part, coefficients varies with incident P-wave angle θ_{P}, scattered S-wave angle θ_{S}, incident P-wave attenuation angle δ_{P}, scattered S-wave attenuation angle δ_{S}. In terms of dependency to medium properties, the inhomogeneous part depends to the anisotropic Thomsen parameters, Q-dependent Thomsen parameters has no influence on this part. In the case that incident wave is homogeneous this terms vanishes. For normal incident wave the anisotropic and homogeneous terms go to zero however the inhomogeneous terms is not zero. In this case only, $\gamma^{(\mathrm{S})}$, $\delta^{(1)}$ and $\delta^{(2)}$ affect the reflection coefficients. Consequently, for incident

inhomogeneous wave the reflection coefficient is given by $\mathrm{R_{PSH}} = \mathrm{R^{AE}_{PSH}} + i\mathrm{R^{H}_{PSH}} + i\mathrm{R^{IH}_{PSH}}$, with the following components

$$\begin{aligned}
\mathrm{R^{AE}_{PSH}} &= \mathrm{A_{PSH1}}\sin\theta_P + \mathrm{A_{PSH2}}\frac{\cos\theta_P\sin\theta_P}{\cos\theta_S} + \mathrm{A_{PSH3}}\sin^3\theta_P + \mathrm{A_{PSH4}}\frac{\cos\theta_P\sin^3\theta_P}{\cos\theta_S},\\
\mathrm{R^{H}_{PSH}} &= \mathrm{A^{H}_{PSH1}}\sin\theta_P + \mathrm{A^{H}_{PSH2}}\frac{\cos\theta_P\sin\theta_P}{\cos\theta_S} + \mathrm{A^{H}_{PSH3}}\sin^3\theta_P + \mathrm{A^{H}_{PSH4}}\frac{\cos\theta_P\sin^3\theta_P}{\cos\theta_S},\\
\mathrm{R^{IH}_{PSH}} &= \mathrm{A^{IH}_{PSH1}} + \mathrm{A^{IH}_{PSH2}}\sin^2\theta_P + \mathrm{A^{IH}_{PSH3}}\sin^4\theta_P,
\end{aligned} \tag{26}$$

with coefficients defined in Appendix A. Here, $\mathrm{R^{AE}_{PSH}}$ is the linearized reflection coefficients for converted P-wave to SH-wave in absence of attenuation in medium (Jílek, 2002b,a). For incident homogenous P-wave in an isotropic-viscoelastic medium reflecting from a viscoelastic-orthorhombic media, the second term added to the reflectivity. Finally, $\mathrm{R^{IH}_{PSH}}$ is the contribution of the inhomogeneity of the wave in reflectivity which is zero when the incident wave is homogeneous. Similar to the PSV-wave, PSH reflection coefficient for normal incident wave is not zero due to the inhomogeneous term $\mathrm{R^{IH}_{PSH}}$. For very small angle of incident, PSH-reflection coefficient varies only with $\gamma^{(\mathrm{S})}$, $\delta^{(S)}$ and corresponding Q-dependant Thomsen parameters $\gamma^{(\mathrm{S})}_{\mathrm{Q}}$ and $\delta^{(S)}_{\mathrm{Q}}$. Neither $\delta^3(\delta^3_Q)$ nor $\varepsilon^{(S)}(\varepsilon^{(S)}_Q)$ affect the reflectivity for small angle of incidence.

DISCUSSION

Determination, by seismic full waveform inversion (FWI), of the anisotropic and attenuative properties of a geological volume, is a challenging task. One of the challenges is that seismic amplitudes are co-determined by the simultaneous variations of several properties, and the separation of these mixing effects is a complex and generally ill-posed problem. To optimally formulate multi-parameter updates in FWI, detailed parameter resolution analysis is required. Quantitative predictions regarding the resolution of any set of parameters can be made based on the scattering radiation patterns generated by local changes in medium parameters. Radiation patterns are computed via the Born approximate model of volume scattering. Scattering amplitudes as a function of opening angle provide information regarding the variations two independent parameters will cause in the data; if they are similar in character over some range of opening angles, one concludes that the two parameters will be difficult to distinguish with data spanning that angle range. For example, within an anisotropic acoustic medium with three parameters, it has been posited that updating the vertical wave velocity with FWI and holding two Thomsen parameters fixed is an optimal choice; however, a parameterization combining two wave velocities and one Thomsen parameter is suitable for wide-azimuth/wide-aperture surface data (Gholami et al., 2013b).

This study is the first effort to establish a framework for parameter resolution analysis for FWI in complex media with both anisotropy and attenuation. Just like any other model parameterization analysis, our approach relies on the Born approximation. We developed radiation pattern formulae for a viscoelastic orthorhombic medium with seven anisotropic Thomsen parameters and seven attenuation-anisotropic parameters. The derived radiation patterns expose to analysis the sensitivity of the scattered wave field the anisotropic parameters in terms of scattering angle. In our analysis, the effects of inhomogeneity, or attenuation angle (the angle between the real and imaginary parts of the wave vector), has been fully taken into account in radiation patterns. The influence of the inhomogeneity angle in regions of high attenuation in (say) unconventional reservoir rocks is not negligible, but its effect on inversion has received almost no attention in the FWI

/ seismic community as yet.

Amplitude variation with offset is normally described using the approximate solutions of the Zoeppritz equations assuming low contrast medium variations. Calculations require determination of slowness and polarization vectors. Exact solutions yield complicated functions in terms of the medium properties describing upper and lower half-spaces as well as incident and transmitted phase angles. Similar results emerge from the Born approximations based on first order perturbation theory. In this paper, using the latter Born approach, scattering potentials and linearized reflection coefficients for a weak anisotropic, low-loss viscoelastic orthorhombic media are derived for P-to-P, P-to-SV and P-to-SH waves. An elastic orthorhombic stiffness tensor is described by nine real independent parameters including vertical P- and S-wave velocities, and seven generalized Thompson parameters which characterize the weak anisotropy in the medium. If attenuation is taken into account, the stiffness tensor components become complex, with imaginary parts related to the associated quality factors and Q-Thompson parameters. In deriving our results, we assume that the background medium is isotropic and viscoelastic, and are perturbed by anisotropic and isotropic-(visco)elastic inclusions. Compared to previously derived converted wave AVAZ equations our derivations are new in two ways. First, we avoid the complications of the solution of Zoeppritz equations by using the Born approximation based on the first order perturbation theory. Second, we obtain extra terms in the AVAz equations due to both the anelasticity of the medium and the inhomogeneity of the wave. We note that the reflection coefficient, which is generally complex, has a real part which is sensitive to the isotropic and anisotropic parameters. For an incident inhomogeneous wave, we show that the approximate reflection coefficients break up into four terms. The first term is real and fully isotropic-elastic, and is sensitive to fractional changes in density and S-wave velocity. The second term, which we have called the homogeneous term is sensitive to the vertical P- and S-wave velocities, P- and S-wave quality factors and anisotropic Thomsen parameters. Third term comes into existence when the incident wave is inhomogeneous, and is sensitive to specifically anisotropic-viscoelastic parameters.

CONCLUSION

Scattering potentials for attenuative anisotropic media provides a simple tool to evaluate the Fréchet kernels, and this is relevant to FWI applications where Fréchet kernels are regarded as a sensitivity kernels. Moreover, the study of scattering potentials highlights the dependency of linearized reflection coefficients to anisotropy and attenuation. Attenuation and anisotropy are essential in amplitude variation with offset (AVO) trends as they changes the amplitude and phase of the scattered wave field from geological interfaces. In this research, we derived the analytic forms of the components of the scattering potentials for scattering of the homogeneous and inhomogeneous waves in attenuative orthrohmobic media. These expressions for scattering potentials which are the sensitivity kernels are involved in building the framework for FWI. Furthermore we showed that how these scattering potentials reduce to the linearized reflection coefficients. We study two cases: first we assume that the wave propagates in the isotropic elastic background medium and scattered by the perturbations in anisotropic orthorhombic media. This is equivalent to the low-contrast media with an incident isotropic elastic media over an anisotropic orthorhombic media. In second case it is assumed that the background medium is isotopic viscoelastic media scattered by the perturbations in attenuative anisotropic orthorhombic media. We show that there is no analytical distinction between the behaviour of the amplitude variation with offset and azimuth for isotropic over anisotropic and anisotropic over anisotropic low-contrast media. Whenever we deal

with the first order approximation, we can use the isotropic polarization and slowness vectors for background medium. This greatly simplifies the analytical expressions, which is complicated by using the analytical form of the polarization and slowness vectors in anisotropic media.

For P-to-P reflection coefficients, it can be seen that for normal incident or zero offset only attenuation in medium affect the P-wave reflection coefficient. Anisotropic-viscoelastic parameters affect the nonnormal incidence part of the reflectivity. Only gradient term is sensitive to the changes in S-wave quality factor, however the changes in P-wave quality factor affects the both intercept and curvature terms. For converted wave, due to the inhomogeneity of the incident wave, in contrast to the elastic case, normal incident reflection coefficient is not zero. As a result we can utilize the inhomogeneous part of the converted wave in AVO/Az to invert the inhomogeneous angle.

We believe the results presented in this paper might be a very fruitful approach to development of the theory of seismic modeling and inversion, especially in the new applications of FWI, such as in identifying quality factors and anisotropic-viscoelastic parameters and improving the imaging of subsurface materials. There are also other avenues to pursue, including any inversion scenario where attenuation presence in anisotropic media. It is useful to inspect the results of scattering potentials to determine whether we can construct a framework for full waveform inversion for a medium with both attenuation and anisotropy.

ACKNOWLEDGMENTS

The authors would like to thank CREWES industrial sponsors and NSERC under the grant CRDPJ 461179-13 for funding this work.

REFERENCES

Aki, K., and Richards, P. G., 2002, Quantitative seismology:

Bai, T., and Tsvankin, I., 2016, Time-domain finite-difference modeling for attenuative anisotropic media: Geophysics, **81**, No. 2, C69–C77.

Bai, T., Tsvankin, I., and Wu, X., 2017, Waveform inversion for attenuation estimation in anisotropic media: Geophysics, **82**, No. 4, WA83–WA93.

Bakulin, A., Grechka, V., and Tsvankin, I., 2000a, Estimation of fracture parameters from reflection seismic dataâĂŤpart i: Hti model due to a single fracture set: Geophysics, **65**, No. 6, 1788–1802.

Bakulin, A., Grechka, V., and Tsvankin, I., 2000b, Estimation of fracture parameters from reflection seismic dataâĂŤpart ii: Fractured models with orthorhombic symmetry: Geophysics, **65**, No. 6, 1803–1817.

Bakulin, A., Grechka, V., and Tsvankin, I., 2000c, Estimation of fracture parameters from reflection seismic dataâĂŤpart iii: Fractured models with monoclinic symmetry: Geophysics, **65**, No. 6, 1818–1830.

Behura, J., and Tsvankin, I., 2009, Role of the inhomogeneity angle in anisotropic attenuation analysis: Geophysics, **74**, No. 5, WB177–WB191.

Beller, S., Monteiller, V., Combe, L., Operto, S., and Nolet, G., 2017, On the sensitivity of teleseismic full-waveform inversion to earth parametrization, initial model and acquisition design: Geophysical Journal International, **212**, No. 2, 1344–1368.

Beylkin, G., and Burridge, R., 1990, Linearized inverse scattering problems in acoustics and elasticity: Wave motion, **12**, No. 1, 15–52.

Borcherdt, R. D., 2009, Viscoelastic waves in layered media: Cambridge University Press.

Burridge, R., Maarten, V., Miller, D., and Spencer, C., 1998, Multiparameter inversion in anisotropic elastic media: Geophysical Journal International, **134**, No. 3, 757–777.

Carcione, J. M., Helle, H. B., and Zhao, T., 1998, Effects of attenuation and anisotropy on reflection amplitude versus offset: Geophysics, **63**, No. 5, 1652–1658.

Castagna, J. P., and Backus, M. M., 1993, Offset-dependent reflectivity - Theory and practice of AVO analysis: Society of Exploration Geophysicists.

Causse, E., Mittet, R., and Ursin, B., 1999, Preconditioning of full-waveform inversion in viscoacoustic media: Geophysics, **64**, No. 1, 130–145.

Chapman, M., Liu, E., and Li, X.-Y., 2006, The influence of fluid sensitive dispersion and attenuation on avo analysis: Geophysical Journal International, **167**, No. 1, 89–105.

Charara, M., Barnes, C., and Tarantola, A., 2000, Full waveform inversion of seismic data for a viscoelastic medium, *in* Methods and applications of inversion, Springer, 68–81.

Chen, H., Innanen, K. A., and Chen, T., 2018, Estimating p-and s-wave inverse quality factors from observed seismic data using an attenuative elastic impedance: Geophysics, **83**, No. 2, R173–R187.

da Silva, N. V., Ratcliffe, A., Vinje, V., and Conroy, G., 2016, A new parameter set for anisotropic multiparameter full-waveform inversion and application to a north sea data set: Geophysics, **81**, No. 4, U25–U38.

Far, M. E., 2011, Seismic characterization of naturally fractured reservoirs: University of Houston.

Far, M. E., and Hardage, B., 2016, Fracture characterization using converted waves: Geophysical Prospecting, **64**, No. 2, 287–298.

Far, M. E., Sayers, C. M., Thomsen, L., Han, D.-h., and Castagna, J. P., 2013a, Seismic characterization of naturally fractured reservoirs using amplitude versus offset and azimuth analysis: Geophysical Prospecting, **61**, No. 2, 427–447.

Far, M. E., Thomsen, L., and Sayers, C. M., 2013b, Seismic characterization of reservoirs with asymmetric fractures: Geophysics, **78**, No. 2, N1–N10.

Fichtner, A., 2010, Full seismic waveform modelling and inversion: Springer Science & Business Media.

Fichtner, A., and van Driel, M., 2014, Models and fréchet kernels for frequency-(in) dependent q: Geophysical Journal International, **198**, No. 3, 1878–1889.

Gholami, Y., Brossier, R., Operto, S., Prieux, V., Ribodetti, A., and Virieux, J., 2013a, Which parameterization is suitable for acoustic vertical transverse isotropic full waveform inversion? part 2: Synthetic and real data case studies from valhall: Geophysics, **78**, No. 2, R107–R124.

Gholami, Y., Brossier, R., Operto, S., Ribodetti, A., and Virieux, J., 2013b, Which parameterization is suitable for acoustic vertical transverse isotropic full waveform inversion? part 1: Sensitivity and trade-off analysis: Geophysics, **78**, No. 2, R81–R105.

Hak, B., and Mulder, W. A., 2011, Seismic attenuation imaging with causality: Geophysical Journal International, **184**, No. 1, 439–451.

He, W., and Plessix, R.-É., 2017, Analysis of different parameterisations of waveform inversion of compressional body waves in an elastic transverse isotropic earth with a vertical axis of symmetry: Geophysical Prospecting, **65**, No. 4, 1004–1024.

Innanen, K. A., 2011, Inversion of the seismic avf/ava signatures of highly attenuative targets: Geophysics, **76**, No. 1, R1–R14.

Innanen, K. A., 2014, Seismic avo and the inverse hessian in precritical reflection full waveform inversion: Geophysical Journal International, **199**, No. 2, 717–734.

Jílek, P., 2002a, Converted ps-wave reflection coefficients in weakly anisotropic media: Pure and Applied Geophysics, **159**, No. 7-8, 1527–1562.

Jílek, P., 2002b, Modeling and inversion of converted-wave reflection coefficients in anisotropic media: A tool for quantitative avo analysis.

Kamath, N., and Tsvankin, I., 2016, Elastic full-waveform inversion for vti media: Methodology and sensitivity analysis: Geophysics, **81**, No. 2, C53–C68.

Kamei, R., and Pratt, R., 2013, Inversion strategies for visco-acoustic waveform inversion: Geophysical Journal International, **194**, No. 2, 859–884.

Keating, S., and Innanen, K. A., 2017, Characterizing and mitigating fwi modeling errors due to uncertainty in attenuation physics, *in* SEG Technical Program Expanded Abstracts 2017, Society of Exploration Geophysicists, 1671–1676.

Levin, V., and Park, J., 1997, P-sh conversions in a flat-layered medium with anisotropy of arbitrary orientation: Geophysical Journal International, **131**, No. 2, 253–266.

Masmoudi, N., and Alkhalifah, T., 2016, A new parameterization for waveform inversion in acoustic orthorhombic mediaorthorhombic parameterization: Geophysics, **81**, No. 4, R157–R171.

Métivier, L., Brossier, R., Operto, S., and Virieux, J., 2015, Acoustic multi-parameter fwi for the reconstruction of p-wave velocity, density and attenuation: preconditioned truncated newton approach, *in* SEG Technical Program Expanded Abstracts 2015, Society of Exploration Geophysicists, 1198–1203.

Moradi, S., and Innanen, K. A., 2015, Scattering of homogeneous and inhomogeneous seismic waves in low-loss viscoelastic media: Geophysical Journal International, **202**, No. 3, 1722–1732.

Moradi, S., and Innanen, K. A., 2016, Viscoelastic amplitude variation with offset equations with account taken of jumps in attenuation angle: Geophysics, **81**, No. 3, N17–N29.

Moradi, S., and Innanen, K. A., 2017, Born scattering and inversion sensitivities in viscoelastic transversely isotropic media: Geophysical Journal International, **211**, No. 2, 1177–1188.

Oh, J.-W., and Alkhalifah, T., 2016a, Elastic orthorhombic anisotropic parameter inversion: An analysis of parameterizationelastic orthorhombic anisotropic fwi: Geophysics, **81**, No. 6, C279–C293.

Oh, J.-W., and Alkhalifah, T., 2016b, The scattering potential of partial derivative wavefields in 3-d elastic orthorhombic media: an inversion prospective: Geophysical Journal International, **206**, No. 3, 1740–1760.

Pan, W., Innanen, K. A., and Geng, Y., 2018, Elastic full-waveform inversion and parametrization analysis applied to walk-away vertical seismic profile data for unconventional (heavy oil) reservoir characterization: Geophysical Journal International, **213**, No. 3, 1934–1968.

Pan, W., Innanen, K. A., Margrave, G. F., Fehler, M. C., Fang, X., and Li, J., 2016, Estimation of elastic constants for hti media using gauss-newton and full-newton multiparameter full-waveform inversion: Geophysics, **81**, No. 5, R275–R291.

Pan, W., Innanen, K. A., and Yuan, Y., 2017, Interparameter tradeoff quantification and reduction in isotropic-elastic full-waveform inversion, *in* SEG Technical Program Expanded Abstracts 2017, Society of Exploration Geophysicists, 1539–1544.

Plessix, R., and Rynja, H., 2010, VTI full waveform inversion: a parameterization study with a narrow azimuth streamer data example, 962–966.

Plessix, R.-E., and Cao, Q., 2011, A parametrization study for surface seismic full waveform inversion in an acoustic vertical transversely isotropic medium: Geophysical Journal International, **185**, No. 1, 539–556.

Ruger, A., 1997, P-wave reflection coefficients for transversely isotropic models with vertical and horizontal axis of symmetry: GEOPHYSICS, **62**, No. 3, 713–722.

Ruger, A., 2002, Reflection Coefficients and Azimuthal AVO Analysis in Anisotropic Media: Society of Exploration Geophysicists.

Samec, P., and Blangy, J. P., 1992, Viscoelastic attenuation, anisotropy, and avo: GEOPHYSICS, **57**, No. 3, 441–450.

Sayers, C. M., 2009, Seismic characterization of reservoirs containing multiple fracture sets: Geophysical Prospecting, **57**, No. 2, 187–192.

Sayers, C. M., and Dean, S., 2001, Azimuth-dependent avo in reservoirs containing non-orthogonal fracture sets: Geophysical Prospecting, **49**, No. 1, 100–106.

Sayers, C. M., and Rickett, J. E., 1997, Azimuthal variation in avo response for fractured gas sands: Geophysical Prospecting, **45**, No. 1, 165–182.

Stolt, R. H., and Weglein, A. B., 2012, Seismic imaging and inversion: application of linear inverse theory: Cambridge University Press.

Tarantola, A., 1986, A strategy for nonlinear elastic inversion of seismic reflection data: GEOPHYSICS, **51**, No. 10, 1893–1903.

Thomsen, L., 1986, Weak elastic anisotropy: GEOPHYSICS, **51**, No. 10, 1954–1966.

Tsvankin, I., 1996, P-wave signatures and notation for transversely isotropic media: An overview: GEOPHYSICS, **61**, No. 2, 467–483.

Tsvankin, I., 1997, Anisotropic parameters and)-wave velocity for orthorhombic media: GEOPHYSICS, **62**, No. 4, 1292–1309.

Tsvankin, I., Gaiser, J., Grechka, V., van der Baan, M., and Thomsen, L., 2010, Seismic anisotropy in exploration and reservoir characterization: An overview: GEOPHYSICS, **75**, No. 5, 75A15–75A29.

Vavrycuk, V., and Psencik, I., 1998, Pp-wave reflection coefficients in weakly anisotropic elastic media: GEOPHYSICS, **63**, No. 6, 2129–2141.

Wu, X., Chapman, M., Li, X.-Y., and Boston, P., 2014, Quantitative gas saturation estimation by frequency-dependent amplitude-versus-offset analysis: Geophysical Prospecting, **62**, No. 6, 1224–1237.

Yang, P., Brossier, R., Metivier, L., and Virieux, J., 2016, A review on the systematic formulation of 3-d multiparameter full waveform inversion in viscoelastic medium: Geophysical Journal International, **207**, No. 1, 129–149.

Zhu, Y., and Tsvankin, I., 2005, Plane-wave attenuation anisotropy in orthorhombic media, 186–189.

APPENDIX A: ANISOTROPIC-VISCOELASTIC THOMSEN PARAMETERS

First let use introduce the Thompson parameters in orthorhombic media introduced by Tsvankin Tsvankin (1997) and Zhu Zhu and Tsvankin (2005)

the VTI parameter ε in the $[x_2, x_3]$ plane

$$\varepsilon^{(1)} = \frac{C_{22} - C_{33}}{2C_{33}}, \tag{27}$$

the VTI parameter δ in the $[x_2, x_3]$ plane

$$\delta^{(1)} = \frac{(C_{23} + C_{44})^2 - (C_{33} - C_{44})^2}{2C_{33}(C_{33} - C_{44})}, \tag{28}$$

the VTI parameter γ in the $[x_2, x_3]$ plane

$$\gamma^{(1)} = \frac{C_{66} - C_{55}}{2C_{55}}, \tag{29}$$

the VTI parameter ε in the symmetry plane $[x_2, x_3]$ normal to the x_2-axis (close to the fractional difference between the P-wave velocities in the x_1- and x_3-directions)

$$\varepsilon^{(2)} = \frac{C_{11} - C_{33}}{2C_{33}}, \tag{30}$$

the VTI parameter δ in the $[x_1, x_3]$ plane (responsible for near-vertical P-wave velocity variations, also influences SV-wave velocity anisotropy)

$$\delta^{(2)} = \frac{(C_{13} + C_{55})^2 - (C_{33} - C_{55})^2}{2C_{33}(C_{33} - C_{55})}, \tag{31}$$

the VTI parameter γ in the $[x_1, x_3]$ plane (close to the fractional difference between the SH-wave velocities

$$\gamma^{(2)} = \frac{C_{66} - C_{44}}{2C_{44}}, \tag{32}$$

the VTI parameter δ in the $[x_1, x_2]$ plane (x_2 is used as the symmetry axis)

$$\delta^{(3)} = \frac{(C_{12} + C_{66})^2 - (C_{11} - C_{66})^2}{2C_{11}(C_{11} - C_{66})}, \tag{33}$$

The same definitions should valid when attenuation is added to the medium. First consider to the complex form of $\varepsilon^{(1)}$

$$\begin{aligned}\hat{\varepsilon}^{(1)} &= \frac{\hat{C}_{22} - \hat{C}_{33}}{2\hat{C}_{33}} = \frac{C_{22}(1 + iQ_{22}^{-1}) - C_{33}(1 + iQ_{33}^{-1})}{2C_{33}(1 + iQ_{33}^{-1})} \\ &= \frac{C_{22}(1 + iQ_{22}^{-1})}{2C_{33}(1 + iQ_{33}^{-1})} - \frac{1}{2} \approx \frac{C_{22}}{2C_{33}}(1 + iQ_{22}^{-1} - iQ_{33}^{-1}) - \frac{1}{2}.\end{aligned}$$

After separation of the real and imaginary parts we arrive at

$$\hat{\varepsilon}^{(1)} = \varepsilon^{(1)} + \frac{i}{2}Q_{33}^{-1}\varepsilon_Q^{(1)},$$

where we defined

$$\varepsilon_Q^{(1)} = \frac{Q_{33} - Q_{22}}{Q_{22}}.$$

Similarly we have

$$\varepsilon_Q^{(2)} = \frac{Q_{33} - Q_{11}}{Q_{11}} \tag{34}$$

$$\delta_Q^{(1)} = 2\frac{C_{23}(C_{23} + C_{44})}{C_{33}(C_{33} - C_{44})}\frac{Q_{33} - Q_{23}}{Q_{23}} + \frac{C_{44}(C_{23} + C_{33})^2}{C_{33}(C_{33} - C_{44})^2}\frac{Q_{33} - Q_{44}}{Q_{44}}, \tag{35}$$

$$\delta_Q^{(2)} = 2\frac{C_{13}(C_{13} + C_{55})}{C_{33}(C_{33} - C_{55})}\frac{Q_{33} - Q_{13}}{Q_{13}} + \frac{C_{55}(C_{13} + C_{33})^2}{C_{33}(C_{33} - C_{55})^2}\frac{Q_{33} - Q_{55}}{Q_{55}}, \tag{36}$$

$$\delta_Q^{(3)} = 2\frac{C_{12}(C_{12} + C_{66})}{C_{11}(C_{11} - C_{66})}\frac{Q_{11} - Q_{12}}{Q_{12}} + \frac{C_{66}(C_{12} + C_{11})^2}{C_{11}(C_{11} - C_{66})^2}\frac{Q_{11} - Q_{66}}{Q_{66}} \tag{37}$$

$$\gamma_Q^{(1)} = \frac{Q_{55} - Q_{66}}{Q_{66}}, \tag{38}$$

$$\gamma_Q^{(2)} = \frac{Q_{44} - Q_{66}}{Q_{66}}, \tag{39}$$

$$\tag{40}$$

APPENDIX B:3D SCATTERING POTENTIAL IN ORTHORHOMBIC MEDIA

Elastic Green's function is a 3×3 tensor that represents the displacement generated by a point source in a certain direction. For example $\mathrm{G}_{pq}(\mathbf{x}, \mathbf{x}')$, is the displacement at location $\mathbf{x}$ in the p direction due to this point force the q direction at location $\mathbf{x}'$. Scattering theory requires the actual medium separated into the background medium and perturbations. Born theory is utilized to model the waves scattered by heterogeneities in medium in terms of the solution of wave equation in background medium. The integral equation for scattered wave in terms of solution in background medium and perturbations is given by the Born approximation (Beylkin and Burridge, 1990)

$$\Delta \mathrm{G}_{pq}(\mathbf{x}_r, \mathbf{x}_s) = \int \mathrm{K}_{\mathrm{pq}}(\mathbf{x}_r, \mathbf{x}_s, \mathbf{x}) d\mathbf{x}, \tag{41}$$

with the Born kernel K_{pq} defined by

$$\mathrm{K}_{\mathrm{pq}}(\mathbf{x}_r, \mathbf{x}_s, \mathbf{x}) = \omega^2 \Delta\rho(\mathbf{x}) \mathrm{G}^0_{ip}(\mathbf{x}_r, \mathbf{x}) \mathrm{G}^0_{iq}(\mathbf{x}, \mathbf{x}_s) - \Delta \mathrm{C}_{ijkl}(\mathbf{x}) \frac{\partial \mathrm{G}^0_{ip}(\mathbf{x}_r, \mathbf{x})}{\partial x_j} \frac{\partial \mathrm{G}^0_{kq}(\mathbf{x}, \mathbf{x}_s)}{\partial x_l}. \tag{42}$$

Where $\Delta \mathrm{G}_{pq} = \mathrm{G}_{pq} - \mathrm{G}^0_{pq}$ is the difference between the Green's function in actual medium G_{pq} and in the background medium G^0_{pq}. Additionally, $\mathbf{x}$ is the location of scatter point, $\mathbf{x}_r$ and $\mathbf{x}_s$ are the location of receiver and source respectively. On the right hand side summation over repeated indices is assumed. $\Delta \mathrm{C}_{ijkl} = \mathrm{C}_{ijkl} - \mathrm{C}^0_{ijkl}$ is the difference between the non-zero components of the stiffness tensor in the actual and the background media; $\mathrm{G}^0_{iq}(\mathbf{x}, \mathbf{x}_s)$ is the Green's function in the background medium responsible for the propagation of the wave from source point $\mathbf{x}_s$ to the point $\mathbf{x}$ where perturbations in density, $\Delta\rho$, and stiffness tensor ΔC_{ijkl} interact with the wavefield, and the Green's function $\mathrm{G}^{(0}_{ip}(\mathbf{x}_r, \mathbf{x})$ delivers the wavefield to the receiver point $\mathbf{x}_r$. To simplify the sensitivity expressions, we write the Green's function in terms of the polarization vectors in source and receiver locations

$$\begin{aligned} \mathrm{G}^{(0)}_{ip}(\mathbf{x}_r, \mathbf{x}) &\sim A(\mathbf{x}, \mathbf{x}_r) \mathcal{S}_i(\mathbf{x}) \mathcal{S}_p(\mathbf{x}_r) e^{i\omega \mathbf{k}^{\mathrm{Sc}} \cdot (\mathbf{x}_r - \mathbf{x})}, \\ \mathrm{G}^{(0)}_{iq}(\mathbf{x}, \mathbf{x}_s) &\sim A(\mathbf{x}, \mathbf{x}_s) \mathcal{I}_i(\mathbf{x}) \mathcal{I}_q(\mathbf{x}_s) e^{i\omega \mathbf{k}^{\mathrm{In}} \cdot (\mathbf{x} - \mathbf{x}_s)}, \end{aligned} \tag{43}$$

where A is a complex amplitude, $\boldsymbol{\mathcal{S}}$ and $\boldsymbol{\mathcal{I}}$ respectively are the polarization vectors of the scattered and incident waves, as defined at the scatter point $\mathbf{x}$, source point $\mathbf{x}_s$ and receiver point $\mathbf{x}_r$. In addition $\mathbf{k}^{\mathrm{Sc}}$ is the slowness vector of the scattered wave field and $\mathbf{k}^{\mathrm{In}}$ is the slowness vector of the incident wavefield. Consequently, the differentiations in the equation (45) can be approximated to

$$\begin{aligned} \frac{\partial \mathrm{G}^{(0)}_{ip}(\mathbf{x}_r, \mathbf{x})}{\partial x_j} &\approx -i\omega \mathrm{k}^{\mathrm{Sc}}_j \mathrm{G}^{(0)}_{ip}(\mathbf{x}_r, \mathbf{x}), \\ \frac{\partial \mathrm{G}^{(0)}_{kq}(\mathbf{x}, \mathbf{x}_s)}{\partial x_l} &\approx i\omega \mathrm{k}^{\mathrm{In}}_l \mathrm{G}^{(0)}_{kq}(\mathbf{x}, \mathbf{x}_s). \end{aligned} \tag{44}$$

then the born kernel reduces to

$$\mathrm{K}_{\mathrm{pq}}(\mathbf{x}_r, \mathbf{x}_s, \mathbf{x}) = \rho_0 \omega^2 A(\mathbf{x}_r, \mathbf{x}) A(\mathbf{x}, \mathbf{x}_s) \mathcal{S}_p(\mathbf{x}_r) [\mathrm{S}(\mathbf{x})] \mathcal{I}_q(\mathbf{x}_s) e^{i\omega \mathbf{k}^{\mathrm{Sc}} \cdot (\mathbf{x}_r - \mathbf{x})} e^{i\omega \mathbf{k}^{\mathrm{In}} \cdot (\mathbf{x} - \mathbf{x}_s)}, \tag{45}$$

where the scattering potential is given by

$$\mathrm{S}(\mathbf{x}) = (\boldsymbol{\mathcal{S}} \cdot \boldsymbol{\mathcal{I}}) \frac{\Delta\rho(\mathbf{x})}{\rho_0(\mathbf{x})} - (\mathcal{S}_i \mathrm{k}^{\mathrm{Sc}}_j \mathcal{I}_k \mathrm{k}^{\mathrm{In}}_l) \frac{\Delta C_{ijkl}(\mathbf{x})}{\rho_0(\mathbf{x})}. \tag{46}$$

Here S is called scattering potential. Furthermore, we can write scattering potentials as

$$\begin{aligned} \rho_0 \mathrm{S} = [\rho]\, \Delta\rho - [C_{11}] \Delta C_{11} - [C_{22}] \Delta C_{22} - [C_{33}] \Delta C_{33} \\ - [C_{12}] \Delta C_{12} - [C_{13}] \Delta C_{13} - [C_{23}] \Delta C_{23} \\ - [C_{44}] \Delta C_{44} - [C_{55}] \Delta C_{55} - [C_{66}] \Delta C_{66}. \end{aligned}$$

Where the sensitivities are

$$
\begin{aligned}
[\rho] &= \boldsymbol{\mathcal{S}} \cdot \boldsymbol{\mathcal{I}}, \\
[C_{11}] &= \mathcal{S}_1 \mathrm{k}_1^{\mathrm{Sc}} \mathcal{I}_1 \mathrm{k}_1^{\mathrm{In}}, \\
[C_{22}] &= \mathcal{S}_2 \mathrm{k}_2^{\mathrm{Sc}} \mathcal{I}_2 \mathrm{k}_2^{\mathrm{In}}, \\
[C_{33}] &= \mathcal{S}_3 \mathrm{k}_3^{\mathrm{Sc}} \mathcal{I}_3 \mathrm{k}_3^{\mathrm{In}}, \\
[C_{12}] &= \mathcal{S}_1 \mathrm{k}_1^{\mathrm{Sc}} \mathcal{I}_2 \mathrm{k}_2^{\mathrm{In}} + \mathcal{S}_2 \mathrm{k}_2^{\mathrm{Sc}} \mathcal{I}_1 \mathrm{k}_1^{\mathrm{In}}, \\
[C_{13}] &= \mathcal{S}_1 \mathrm{k}_1^{\mathrm{Sc}} \mathcal{I}_3 \mathrm{k}_3^{\mathrm{In}} + \mathcal{S}_3 \mathrm{k}_3^{\mathrm{Sc}} \mathcal{I}_1 \mathrm{k}_1^{\mathrm{In}}, \\
[C_{23}] &= \mathcal{S}_2 \mathrm{k}_2^{\mathrm{Sc}} \mathcal{I}_3 \mathrm{k}_3^{\mathrm{In}} + \mathcal{S}_3 \mathrm{k}_3^{\mathrm{Sc}} \mathcal{I}_2 \mathrm{k}_2^{\mathrm{In}}, \\
[C_{44}] &= \mathcal{S}_2 \mathrm{k}_3^{\mathrm{Sc}} \mathcal{I}_2 \mathrm{k}_3^{\mathrm{In}} + \mathcal{S}_3 \mathrm{k}_2^{\mathrm{Sc}} \mathcal{I}_2 \mathrm{k}_3^{\mathrm{In}} + \mathcal{S}_2 \mathrm{k}_3^{\mathrm{Sc}} \mathcal{I}_3 \mathrm{k}_2^{\mathrm{In}} + \mathcal{S}_3 \mathrm{k}_2^{\mathrm{Sc}} \mathcal{I}_3 \mathrm{k}_2^{\mathrm{In}}, \\
[C_{55}] &= \mathcal{S}_1 \mathrm{k}_3^{\mathrm{Sc}} \mathcal{I}_1 \mathrm{k}_3^{\mathrm{In}} + \mathcal{S}_3 \mathrm{k}_1^{\mathrm{Sc}} \mathcal{I}_3 \mathrm{k}_1^{\mathrm{In}} + \mathcal{S}_3 \mathrm{k}_1^{\mathrm{Sc}} \mathcal{I}_1 \mathrm{k}_3^{\mathrm{In}} + \mathcal{S}_1 \mathrm{k}_3^{\mathrm{Sc}} \mathcal{I}_3 \mathrm{k}_1^{\mathrm{In}}, \\
[C_{66}] &= \mathcal{S}_1 \mathrm{k}_2^{\mathrm{Sc}} \mathcal{I}_1 \mathrm{k}_2^{\mathrm{In}} + \mathcal{S}_2 \mathrm{k}_1^{\mathrm{Sc}} \mathcal{I}_2 \mathrm{k}_1^{\mathrm{In}} + \mathcal{S}_2 \mathrm{k}_1^{\mathrm{Sc}} \mathcal{I}_1 \mathrm{k}_2^{\mathrm{In}} + \mathcal{S}_1 \mathrm{k}_2^{\mathrm{Sc}} \mathcal{I}_2 \mathrm{k}_1^{\mathrm{In}}.
\end{aligned}
$$

APPENDIX C: AVO COEFFICIENTS

For converted PSV-wave, coefficients for the anisotropic-elastic part in $\mathrm{R}_{\mathrm{PSV}}^{\mathrm{AE}}$ (eq. 23) are given by

$$
\begin{aligned}
\mathrm{A}_{\mathrm{PSV1}}^{\mathrm{AE}} =& \frac{V_P^2}{2(V_P^2 - V_S^2)} \Delta_{12}, \\
\mathrm{A}_{\mathrm{PSV2}}^{\mathrm{AE}} =& -2 \frac{V_S}{V_P} \Gamma_{\mathrm{S}} - \frac{V_S V_P}{2(V_P^2 - V_S^2)} \Delta_{12}, \\
\mathrm{A}_{\mathrm{PSV3}}^{\mathrm{AE}} =& 2 \frac{V_S^2}{V_P^2} \Gamma_{\mathrm{S}} - \frac{V_S^2}{2(V_P^2 - V_S^2)} \Delta_{12} - \frac{V_P^2}{(V_P^2 - V_S^2)} (\Delta_{123} - \Sigma), \\
\mathrm{A}_{\mathrm{PSV4}}^{\mathrm{AE}} =& \frac{V_S V_P}{(V_P^2 - V_S^2)} (\Delta_{123} - \Sigma), \\
\mathrm{A}_{\mathrm{PSV5}}^{\mathrm{AE}} =& \frac{V_S^2}{(V_P^2 - V_S^2)} (\Delta_{123} - \Sigma),
\end{aligned}
$$

where

$$
\begin{aligned}
\Delta_{12} &= \sin^2 \varphi \delta^{(1)} + \cos^2 \varphi \delta^{(2)}, \\
\Gamma_{\mathrm{S}} &= \gamma^{(S)} \sin^2 \varphi, \\
\Delta_{123} &= \sin^2 \varphi \delta^{(1)} + \cos^2 \varphi \delta^{(2)} - \sin^2 \varphi \cos^2 \varphi \delta^{(3)}, \\
\Sigma &= \sin^4 \varphi \varepsilon^{(1)} + \left(\cos^4 \varphi + 2 \cos^2 \varphi \sin^2 \varphi \right) \varepsilon^{(2)}.
\end{aligned}
$$

For homogeneous term $\mathrm{R}^{\mathrm{H}}_{\mathrm{PSV}}$ (eq. 24) coefficients are given by

$$
\begin{aligned}
\mathrm{A}^{\mathrm{H}}_{\mathrm{PSV1}} =& \mathrm{Q}_{\mathrm{P}}^{-1}\frac{1}{4}\frac{\mathrm{V}_{\mathrm{P}}^2}{(\mathrm{V}_{\mathrm{P}}^2-\mathrm{V}_{\mathrm{S}}^2)}\Delta_{Q12}+(\mathrm{Q}_{\mathrm{S}}^{-1}-\mathrm{Q}_{\mathrm{P}}^{-1})\frac{\mathrm{V}_{\mathrm{P}}^2\mathrm{V}_{\mathrm{S}}^2}{2(\mathrm{V}_{\mathrm{P}}^2-\mathrm{V}_{\mathrm{S}}^2)^2}\Delta_{12},\\
\mathrm{A}^{\mathrm{H}}_{\mathrm{PSV2}} =& -\mathrm{Q}_{\mathrm{S}}^{-1}\frac{\mathrm{V}_{\mathrm{S}}}{\mathrm{V}_{\mathrm{P}}}\Gamma_{\mathrm{QS}}-(\mathrm{Q}_{\mathrm{S}}^{-1}-\mathrm{Q}_{\mathrm{P}}^{-1})\frac{\mathrm{V}_{\mathrm{S}}}{\mathrm{V}_{\mathrm{P}}}\Gamma_{\mathrm{S}}-\mathrm{Q}_{\mathrm{P}}^{-1}\frac{\mathrm{V}_{\mathrm{S}}\mathrm{V}_{\mathrm{P}}}{4(\mathrm{V}_{\mathrm{P}}^2-\mathrm{V}_{\mathrm{S}}^2)}\Delta_{\mathrm{Q12}}\\
&-\frac{\mathrm{V}_{\mathrm{S}}\mathrm{V}_{\mathrm{P}}}{4(\mathrm{V}_{\mathrm{P}}^2-\mathrm{V}_{\mathrm{S}}^2)}\left[(\mathrm{Q}_{\mathrm{S}}^{-1}+\mathrm{Q}_{\mathrm{P}}^{-1})+2\frac{\mathrm{V}_{\mathrm{S}}^2\mathrm{Q}_{\mathrm{S}}^{-1}-\mathrm{V}_{\mathrm{P}}^2\mathrm{Q}_{\mathrm{P}}^{-1}}{\mathrm{V}_{\mathrm{P}}^2-\mathrm{V}_{\mathrm{S}}^2}\right]\Delta_{12},\\
\mathrm{A}^{\mathrm{H}}_{\mathrm{PSV3}} =& \mathrm{Q}_{\mathrm{S}}^{-1}\frac{\mathrm{V}_{\mathrm{S}}^2}{\mathrm{V}_{\mathrm{P}}^2}\Gamma_{\mathrm{QS}}+2(\mathrm{Q}_{\mathrm{S}}^{-1}-\mathrm{Q}_{\mathrm{P}}^{-1})\frac{\mathrm{V}_{\mathrm{S}}^2}{\mathrm{V}_{\mathrm{P}}^2}\Gamma_{\mathrm{S}}-\mathrm{Q}_{\mathrm{P}}^{-1}\frac{\mathrm{V}_{\mathrm{S}}^2}{4(\mathrm{V}_{\mathrm{P}}^2-\mathrm{V}_{\mathrm{S}}^2)}\Delta_{\mathrm{Q12}}\\
&-(\mathrm{Q}_{\mathrm{S}}^{-1}-\mathrm{Q}_{\mathrm{P}}^{-1})\frac{\mathrm{V}_{\mathrm{P}}^2\mathrm{V}_{\mathrm{S}}^2}{2(\mathrm{V}_{\mathrm{P}}^2-\mathrm{V}_{\mathrm{S}}^2)^2}\Delta_{12}-\mathrm{Q}_{\mathrm{P}}^{-1}\frac{\mathrm{V}_{\mathrm{P}}^2}{2(\mathrm{V}_{\mathrm{P}}^2-\mathrm{V}_{\mathrm{S}}^2)}\Delta_{Q123}\\
&-(\mathrm{Q}_{\mathrm{S}}^{-1}-\mathrm{Q}_{\mathrm{P}}^{-1})\frac{\mathrm{V}_{\mathrm{P}}^2\mathrm{V}_{\mathrm{S}}^2}{(\mathrm{V}_{\mathrm{P}}^2-\mathrm{V}_{\mathrm{S}}^2)^2}\Delta_{123}+\mathrm{Q}_{\mathrm{P}}^{-1}\frac{\mathrm{V}_{\mathrm{P}}^2}{2(\mathrm{V}_{\mathrm{P}}^2-\mathrm{V}_{\mathrm{S}}^2)}\Sigma_{\mathrm{Q}}\\
&+(\mathrm{Q}_{\mathrm{S}}^{-1}-\mathrm{Q}_{\mathrm{P}}^{-1})\frac{\mathrm{V}_{\mathrm{P}}^2\mathrm{V}_{\mathrm{S}}^2}{(\mathrm{V}_{\mathrm{P}}^2-\mathrm{V}_{\mathrm{S}}^2)^2}\Sigma,\\
\mathrm{A}^{\mathrm{H}}_{\mathrm{PSV4}} =& \frac{1}{2}\mathrm{Q}_{\mathrm{P}}^{-1}\frac{\mathrm{V}_{\mathrm{S}}\mathrm{V}_{\mathrm{P}}}{(\mathrm{V}_{\mathrm{P}}^2-\mathrm{V}_{\mathrm{S}}^2)}\Delta_{\mathrm{Q123}}-\frac{\mathrm{V}_{\mathrm{S}}\mathrm{V}_{\mathrm{P}}}{2(\mathrm{V}_{\mathrm{P}}^2-\mathrm{V}_{\mathrm{S}}^2)}\left[(\mathrm{Q}_{\mathrm{S}}^{-1}+\mathrm{Q}_{\mathrm{P}}^{-1})+2\frac{\mathrm{V}_{\mathrm{S}}^2\mathrm{Q}_{\mathrm{S}}^{-1}-\mathrm{V}_{\mathrm{P}}^2\mathrm{Q}_{\mathrm{P}}^{-1}}{\mathrm{V}_{\mathrm{P}}^2-\mathrm{V}_{\mathrm{S}}^2}\right]\Delta_{123}\\
&-\frac{1}{2}\mathrm{Q}_{\mathrm{P}}^{-1}\frac{\mathrm{V}_{\mathrm{S}}\mathrm{V}_{\mathrm{P}}}{(\mathrm{V}_{\mathrm{P}}^2-\mathrm{V}_{\mathrm{S}}^2)}\Sigma_{\mathrm{Q}}+\frac{\mathrm{V}_{\mathrm{S}}\mathrm{V}_{\mathrm{P}}}{2(\mathrm{V}_{\mathrm{P}}^2-\mathrm{V}_{\mathrm{S}}^2)}\left[(\mathrm{Q}_{\mathrm{S}}^{-1}+\mathrm{Q}_{\mathrm{P}}^{-1})+2\frac{\mathrm{V}_{\mathrm{S}}^2\mathrm{Q}_{\mathrm{S}}^{-1}-\mathrm{V}_{\mathrm{P}}^2\mathrm{Q}_{\mathrm{P}}^{-1}}{\mathrm{V}_{\mathrm{P}}^2-\mathrm{V}_{\mathrm{S}}^2}\right]\Sigma,\\
\mathrm{A}^{\mathrm{H}}_{\mathrm{PSV5}} =& \frac{1}{2}\mathrm{Q}_{\mathrm{P}}^{-1}\frac{\mathrm{V}_{\mathrm{S}}^2}{(\mathrm{V}_{\mathrm{P}}^2-\mathrm{V}_{\mathrm{S}}^2)}\Delta_{Q12}+(\mathrm{Q}_{\mathrm{S}}^{-1}-\mathrm{Q}_{\mathrm{P}}^{-1})\frac{\mathrm{V}_{\mathrm{P}}^2\mathrm{V}_{\mathrm{S}}^2}{(\mathrm{V}_{\mathrm{P}}^2-\mathrm{V}_{\mathrm{S}}^2)^2}\Delta_{12}\\
&-\frac{1}{2}\mathrm{Q}_{\mathrm{P}}^{-1}\frac{\mathrm{V}_{\mathrm{S}}^2}{(\mathrm{V}_{\mathrm{P}}^2-\mathrm{V}_{\mathrm{S}}^2)}\Sigma_{\mathrm{Q}}-(\mathrm{Q}_{\mathrm{S}}^{-1}-\mathrm{Q}_{\mathrm{P}}^{-1})\frac{\mathrm{V}_{\mathrm{P}}^2\mathrm{V}_{\mathrm{S}}^2}{(\mathrm{V}_{\mathrm{P}}^2-\mathrm{V}_{\mathrm{S}}^2)^2}\Sigma,
\end{aligned}
$$

where

$$
\begin{aligned}
\Delta_{Q12} &= \sin^2\varphi\delta_{\mathrm{Q}}^{(1)}+\cos^2\varphi\delta_{\mathrm{Q}}^{(2)},\\
\Gamma_{\mathrm{QS}} &= \gamma_{\mathrm{Q}}^{(S)}\sin^2\varphi,\\
\Delta_{Q123} &= \sin^2\varphi\delta_{\mathrm{Q}}^{(1)}+\cos^2\varphi\delta_{\mathrm{Q}}^{(2)}-\sin^2\varphi\cos^2\varphi\delta_{\mathrm{Q}}^{(3)},\\
\Sigma_{\mathrm{Q}} &= \sin^4\varphi\varepsilon_{\mathrm{Q}}^{(1)}+\left(\cos^4\varphi+2\cos^2\varphi\sin^2\varphi\right)\varepsilon_{\mathrm{Q}}^{(2)}.
\end{aligned}
$$

For homogeneous term $\mathrm{R}^{\mathrm{IH}}_{\mathrm{PSV}}$ (eq. 25) coefficients are given by

$$
\begin{aligned}
\mathrm{A}^{\mathrm{IH}}_{\mathrm{PSV1}} =& \frac{1}{2}Q_P^{-1}\tan\delta_P\left[A_{\mathrm{PSV1}}\frac{\cos\theta_P}{\cos\theta_S}+A_{\mathrm{PSV2}}\right],\\
\mathrm{A}^{\mathrm{IH}}_{\mathrm{PSV2}} =& \left[\frac{Q_S^{-1}}{2}\mathrm{V}_{\mathrm{SP}}A_{\mathrm{PSV1}}\tan\delta_S\right]\frac{1}{\cos^2\theta_S}-\tan\delta_P Q_P^{-1}\left[A_{\mathrm{PSV2}}+\frac{1}{2}A_{\mathrm{PSV3}}\right]\frac{\cos\theta_P}{\cos\theta_S}\\
&+Q_P^{-1}\tan\delta_P\left[\frac{3}{2}A_{\mathrm{PSV4}},+A_{\mathrm{PSV3}}\frac{\cos\theta_P}{\cos\theta_S}\right]\sin^2\theta_P,\\
\mathrm{A}^{\mathrm{IH}}_{\mathrm{PSV3}} =& \frac{Q_S^{-1}}{2}\mathrm{V}_{\mathrm{SP}}A_{\mathrm{PSV3}}\tan\delta_S\frac{1}{\cos^2\theta_S}-Q_P^{-1}\tan\delta_P\left[2A_{\mathrm{PSV4}}+\frac{5}{4}A_{\mathrm{PSV5}}\frac{\cos\theta_P}{\cos\theta_S}\right],\\
\mathrm{A}^{\mathrm{IH}}_{\mathrm{PSV4}} =& \left[\frac{Q_S^{-1}}{2}\mathrm{V}_{\mathrm{SP}}A_{\mathrm{PSV5}}\tan\delta_S\frac{1}{\cos^2\theta_S}\right].
\end{aligned}
$$

For converted PSH-wave, coefficients for the anisotropic-elastic part in $\mathrm{R}^{\mathrm{AE}}_{\mathrm{PSH}}$ (eq. 26) are given by

$$
\begin{aligned}
\mathrm{A}^{\mathrm{AE}}_{\mathrm{PSH1}} =& -\frac{V_P^2}{4(V_P^2-V_S^2)}\sin 2\varphi\delta^{(S)},\\
\mathrm{A}^{\mathrm{AE}}_{\mathrm{PSH2}} =& \frac{V_S}{V_P}\sin 2\varphi\gamma^{(S)} + \frac{V_P V_S}{4(V_P^2-V_S^2)}\sin 2\varphi\delta^{(S)},\\
\mathrm{A}^{\mathrm{AE}}_{\mathrm{PSH3}} =& \frac{V_P^2}{4(V_P^2-V_S^2)}\sin 2\varphi\left[\delta^{(S)} + \left(\sin^2\varphi - \cos^2\varphi\right)\delta^{(3)} - 2\sin^2\varphi\varepsilon^{(S)}\right],\\
\mathrm{A}^{\mathrm{AE}}_{\mathrm{PSH4}} =& -\frac{V_S V_P}{4(V_P^2-V_S^2)}\sin 2\varphi\left[\delta^{(S)} + \left(\sin^2\varphi - \cos^2\varphi\right)\delta^{(3)} - 2\sin^2\varphi\varepsilon^{(S)}\right].
\end{aligned}
$$

For homogeneous term $\mathrm{R}^{\mathrm{H}}_{\mathrm{PSH}}$ coefficients are given by

$$
\begin{aligned}
\mathrm{A}^{\mathrm{H}}_{\mathrm{PSH1}} =& -\mathrm{Q}_{\mathrm{P}}^{-1}\frac{\mathrm{V}_{\mathrm{P}}^2}{8(\mathrm{V}_{\mathrm{P}}^2-\mathrm{V}_{\mathrm{S}}^2)}\sin 2\varphi\delta_Q^{(S)} - (\mathrm{Q}_{\mathrm{S}}^{-1}-\mathrm{Q}_{\mathrm{P}}^{-1})\frac{\mathrm{V}_{\mathrm{P}}^2\mathrm{V}_{\mathrm{S}}^2}{4(\mathrm{V}_{\mathrm{P}}^2-\mathrm{V}_{\mathrm{S}}^2)^2}\sin 2\varphi\delta^{(S)},\\
\mathrm{A}^{\mathrm{H}}_{\mathrm{PSH2}} =& \frac{1}{2}\mathrm{Q}_{\mathrm{S}}^{-1}\frac{V_S}{V_P}\sin 2\varphi\gamma_Q^{(S)} + \frac{1}{2}(\mathrm{Q}_{\mathrm{S}}^{-1}-\mathrm{Q}_{\mathrm{P}}^{-1})\frac{V_S}{V_P}\sin 2\varphi\gamma^{(S)} + \mathrm{Q}_{\mathrm{P}}^{-1}\frac{V_P V_S}{8(V_P^2-V_S^2)}\sin 2\varphi\delta_Q^{(S)},\\
&+ \frac{V_S V_P}{8(V_P^2-V_S^2)}\left[(\mathrm{Q}_{\mathrm{S}}^{-1}+\mathrm{Q}_{\mathrm{P}}^{-1}) + 2\frac{V_S^2\mathrm{Q}_{\mathrm{S}}^{-1} - V_P^2\mathrm{Q}_{\mathrm{P}}^{-1}}{V_P^2-V_S^2}\right]\sin 2\varphi\delta^{(S)},\\
\mathrm{A}^{\mathrm{H}}_{\mathrm{PSH3}} =& \mathrm{Q}_{\mathrm{P}}^{-1}\frac{V_P^2}{8(V_P^2-V_S^2)}\sin 2\varphi\left[\delta_Q^{(S)} - 2\sin^2\varphi\varepsilon_Q^{(S)} + \left(\sin^2\varphi-\cos^2\varphi\right)\delta_Q^{(3)}\right],\\
&+ (\mathrm{Q}_{\mathrm{S}}^{-1}-\mathrm{Q}_{\mathrm{P}}^{-1})\frac{V_P^2 V_S^2}{8(V_P^2-V_S^2)^2}\sin 2\varphi\left[\delta^{(S)} - 2\sin^2\varphi\varepsilon^{(S)} + \left(\sin^2\varphi-\cos^2\varphi\right)\delta^{(3)}\right],\\
\mathrm{A}^{\mathrm{H}}_{\mathrm{PSH4}} =& -\mathrm{Q}_{\mathrm{P}}^{-1}\frac{V_S V_P}{8(V_P^2-V_S^2)}\sin 2\varphi\left[\delta_Q^{(S)} - 2\sin^2\varphi\varepsilon_Q^{(S)} + \left(\sin^2\varphi-\cos^2\varphi\right)\delta_Q^{(3)}\right],\\
&- \frac{V_S V_P}{8(V_P^2-V_S^2)}\left[(\mathrm{Q}_{\mathrm{S}}^{-1}+\mathrm{Q}_{\mathrm{P}}^{-1}) + 2\frac{V_S^2\mathrm{Q}_{\mathrm{S}}^{-1} - V_P^2\mathrm{Q}_{\mathrm{P}}^{-1}}{V_P^2-V_S^2}\right]\times\\
&\sin 2\varphi\left[\delta^{(S)} - 2\sin^2\varphi\varepsilon^{(S)} + \left(\sin^2\varphi-\cos^2\varphi\right)\delta^{(3)}\right].
\end{aligned}
$$

For inhomogeneous term $\mathrm{R}^{\mathrm{IH}}_{\mathrm{PSH}}$ coefficients are given by

$$
\begin{aligned}
\mathrm{A}^{\mathrm{IH}}_{\mathrm{PSH1}} =& \frac{1}{2}Q_P^{-1}\tan\delta_P\left[A_{\mathrm{PSH1}}\cos\theta_P + A_{\mathrm{PSH2}}\frac{1}{\cos\theta_S}\right],\\
\mathrm{A}^{\mathrm{IH}}_{\mathrm{PSH2}} =& -\frac{1}{2}A_{\mathrm{PSH2}}\left\{Q_P^{-1}\tan\delta_P\left[\frac{\cos\theta_P}{\cos\theta_S} + \frac{1}{\cos\theta_S}\right] + \left[Q_S^{-1}\mathrm{V_{SP}}\tan\delta_S\right]\frac{1}{\cos^2\theta_S}\right\}\\
&+ \frac{3}{2}Q_P^{-1}\tan\delta_P\left[A_{\mathrm{PSH3}}\cos\theta_P + A_{\mathrm{PSH4}}\frac{1}{\cos\theta_S}\right],\\
\mathrm{A}^{\mathrm{IH}}_{\mathrm{PSH3}} =& A_{\mathrm{PSH4}}\left[\frac{Q_S^{-1}}{2}\mathrm{V_{SP}}\tan\delta_S\frac{\cos\theta_P}{\cos^2\theta_S} - 2Q_P^{-1}\tan\delta_P\frac{1}{\cos\theta_S}\right].
\end{aligned}
$$